Chemical Engineering Journal 449 (2022) 137810

Contents lists available at ScienceDirect

Chemical Engineering Journal

journal homepage: www.elsevier.com/locate/cej

A novel 'sea-thermal', synergistic co-valorisation approach for biofuels production from unavoidable food waste (almond hulls) and plastic residues (disposable face masks)

Javier Remón [a,*], Gonzalo Zapata [a], Luis Oriol [b,c], José Luis Pinilla [a], Isabel Suelves [a]

[a] Instituto de Carboquímica, CSIC. C/Miguel Luesma Castán 4, 50018 Zaragoza, Spain
[b] Departamento de Química Orgánica, Facultad de Ciencias, Universidad de Zaragoza, Pedro Cerbuna 12, 50009 Zaragoza, Spain
[c] Instituto de Nanociencia y Materiales de Aragón (INMA), CSIC-Universidad de Zaragoza, 50009 Zaragoza, Spain

ARTICLE INFO

Keywords:
Almond hulls
Disposable face masks
Co-valorisation
Feedstock interactions
Seawater

ABSTRACT

This work first-time addresses the synergetic hydrothermal co-valorisation of almond hulls (an unavoidable food waste) and FFP2 face masks (a common plastic material) using seawater (a sustainable reaction medium). The effects of the feedstock composition (each material alone and all possible binary combinations) and the reaction medium (deionised water, seawater and all possible binary mixtures) have been evaluated at 350 °C and 170 bar over a wide range of reaction times (20–180 min). Bilateral biomass-plastic synergistic and antagonistic interactions between both feedstocks, combined with several promoting and inhibiting effects displayed by seawater, ruled the distribution of the reaction products and their most important physicochemical and fuel properties. Process optimisation revealed that the formation of an energy-dense (32 MJ/kg) liquid biofuel was maximised (26% biocrude yield) by conducting the process with almond hulls in deionised water for 115 min. At the same time, face masks promoted solid biofuel formation (83% hydrochar yield, 46 MJ/kg) by coprocessing an almond hulls/disposable face masks mixture (8:92 wt%) in salted (seawater/deionised water mixture with 37471 ppm salinity) water for 180 min. Conducting the process with seawater (44608 ppm salinity) for 180 min allowed coprocessing of both materials (22/78 wt% almond hulls/face masks) efficiently to maximise biofuels production (13% biocrude yield, HHV = 33 MJ/kg and 67% hydrochar yield, HHV = 49 MJ/kg). These results are a breakthrough in developing season-free and flexible biorefineries, which contribute to reducing pollution and bringing out the hidden value of human activity common residues.

1. Introduction

The ongoing movement to replace the present fossil-based chemistry and energy sectors with a bio-renewable energy market has led researchers to explore alternative bio-based feedstocks and develop novel and more sustainable processes for the production of fuels and chemicals. Apart from a sustainable production, it is also essential to deal with residues causing environmental concerns to ensure the welfare of present and future generations. Thus, a significant effort must be put into finding innovative solutions to add value to such wastes [1]. This new policy ensures re-utilisation following a circular economy approach and helps preserve ecosystems to guarantee the well-being of the planet. With this in mind, earth and sea industrial by-products and wastes can be regarded as promising and alternative materials to furnish an extensive range of biofuels and biochemicals by means of a waste to wealth strategy [1,2].

Two common terrestrial and marine residues are unavoidable food waste and plastic residues. Unavoidable food waste is a common by-product produced in large quantities on the earth. As one way to improve food security is by decreasing food waste to reduce environmental impacts, it is necessary to develop sustainable processes for its efficient management. Among the different types of unavoidable lignocellulosic food wastes, almond hulls, produced as a by-product in the almond processing industry, are excellent candidates for developing novel biorefineries. The almond hull is the outer covering of the almond kernel and shell and accounts for more than half of the total almond weight [3]. Its production has increased dramatically over the past few years due to the recent increase in almonds production globally (e.g.

* Corresponding author.
E-mail address: jremon@icb.csic.es (J. Remón).

https://doi.org/10.1016/j.cej.2022.137810

Available online 27 June 2022

worldwide production has risen from 0.7 Mt in 2007 to 1.5 Mt in 2020 [4]). In parallel, waste plastics are currently one of the most concerning terrestrial and seawater pollution forms. These plastics are present in landfilled municipal solid waste (MSW), mixed with food waste, yard trimmings, paper, wood and leather [5]. Besides, recent studies estimate that more than 5 trillion of plastic particles are afloat in the ocean, accounting for around 300 000 tonnes of plastic matter [6]. These marine plastics primarily originate from single-use packaging, plastic drink bottles and polyethylene bags [6]. The recent COVID-19 pandemic caused by the SARS CoV-2 virus has compounded this issue owing to the increase in the production and disposal of protective plastic materials, such as face masks, protection screens, hoses and coats. Among these, the use and disposal of face masks have substantially risen as they are globally used [7]. These masks consist of three distinctive parts: filter, nose wire and ear strap. The filter accounts for more than 95 wt% of the material and comprises polypropylene and polyethylene [7]. The management and recycling of these masks are complex as there is a high biological contamination risk. While individual collection points could be placed at hospitals, masks used by the population are not collected individually.

Taking the chemical nature of these feedstocks into account, thermochemical processes are suitable for the individual and joint valorisation of lignocellulosic food waste and plastics [8]. Mainly, pyrolysis, gasification and hydrothermal treatments have gained widespread interest in producing energy-dense fuels and valuable chemicals from these materials. Pyrolysis and gasification have been widely used for biomass valorisation, and recently Jung et al. [7] published the first work studying the pyrolysis of FFP2 masks for biofuel production. Hydrothermal treatment (HTT) is also regarded as an excellent candidate for the management and valorisation of bio- (biomass) and synthetic (plastics) polymers. HTT is conducted in the liquid phase at subcritical conditions, i.e., temperatures between 150 and 374 °C and pressures from 5 to 22 MPa [9,10]. As a result, a liquid organic product (biocrude), an aqueous fraction, a gas stream and a solid spent product (hydrochar) are typically produced, with the yields and properties of these fractions depending on the processing conditions and feedstock [9,10]. One of the principal advantages of HTT is that the processing conditions dispense with the need to vaporise the water and/or dry the raw material, which improves the economic aspects and energetic profitability of the process. Besides, it uses lower temperatures and produces biofuels with better physicochemical and fuel properties than those produced via pyrolysis [9,11–15].

Accounting for these excellent features, the use of HTTs for the valorisation of lignocellulosic and plastic materials is receiving increasing attention. Despite there is a substantial amount of work reporting on the HTT of lignocellulosic agricultural wastes [16,17], such as swine manure [18], artificial garbage [19], sawdust, rice husk [20] and beech wood [21], publications addressing the HTT of unavoidable food waste in general or almond hulls, in particular, are very scarce. In a previous publication [22], we addressed the valorisation and management of almond hulls, scrutinising the effect of the processing conditions (temperature, pressure, time and solid/water ratio). The experimental results revealed that HTT is a promising route to develop holistic biorefineries to produce biofuels (biocrude and hydrochar) and value-added chemicals (saccharide-rich aqueous solutions) concurrently [22]. On the contrary, the use of HTTs for the valorisation and management of plastics is at an early development stage. In fact, publications are very scarce and only address the HTT of different types of plastics individually, such as polystyrene [23], polycarbonate [24], polybutylene terephthalate, polycarbonate, polyethylene terephthalate, polylactic acid, polymethyl methacrylate, polyoxymethylene, poly-p-phenylene oxide, polyvinyl alcohol, styrene-butadiene [25], along with comparisons between the behaviour of polypropylene, polystyrene, polycarbonate and polyethylene terephthalate [26]. Thus, the HTT of disposable face protective masks, mainly composed of polypropylene and polyethylene, is not yet reported to the best of the authors' knowledge.

Work conducted on the HTT of biomass and plastic has highlighted that their different chemical structures significantly influence the process, which results in specific processing conditions for each material. For example, most plastics decompose between 350 and 450 °C, while lignocellulosic biomass depolymerises between 250 and 350 °C, which may hamper the coprocessing of both materials [26]. On the bright side, it has been recently reported that the addition of biomass to plastic can reduce the decomposition temperature of the latter, which increases the overall yields due to synergistic effects [27–30]. Besides, some plastic, such as polyethylene and polypropylene, can act as a hydrogen source to increase the biocrude yield and enhance its fuel properties [31,32]. This aligns with new biorefinery principles and opens the door to transition from single feedstock dependent processes to 'feedstock independent', 'season-free', holistic biorefineries [33,34]. Regarding biomass and plastic synergistic processes, Yuan et al. [30] reported that the biocrude yield obtained from the HTT of an 80/20 (wt.%) high-density polyethylene/sawdust was 8 times higher than the yields produced from both materials individually. In addition, synergistic effects were also reported for polyethylene terephthalate/lignin [29] and polyethylene terephthalate/wheat straw [27], polyethylene terephthalate/pistachio shells [6] and polypropylene/microalgae [28]. These interactions were pivotal to decreasing the processing temperature of plastic materials under hydrothermal conditions. Very recently, Seshasayee et al. [5] studied the hydrothermal co-valorisation at 300–425 °C of different biomasses (cellulose, lignin, starch, soy protein, stearic acid and municipal solid waste) with several plastics (polystyrene, polypropylene, polycarbonate and polyethylene terephthalate). They reported that cellulose, starch and lignin synergistically interacted with mixtures of polypropylene, polycarbonate, polystyrene and polyethylene terephthalate. These interactions increased the biocrude yield and enabled the process to be conducted at lower temperatures.

For the future development and commercialisation of synergistic and holistic biorefineries, finding appropriate catalysts for each process within the different units is also paramount. During HTTs, subcritical water behaves simultaneously as a solvent, reactant and catalyst for a substantial number of depolymerisation and repolymerisation reactions occurring in the process, and many works have been published in the absence of a catalyst [5,11,14]. Still, the addition of homogeneous or heterogeneous catalysts has also been studied to increase the yields and enhance the properties of key products (biocrude and hydrochar) [35]. The former largely comprise alkali salts such as Na_2CO_3, K_2CO_3 and $KHCO_3$ [6,13]. These salts help to reduce char formation and improve the properties of the biocrude by promoting the water–gas shift, dehydration and deoxygenation reactions [6,13]. The latter comprise metals (Pt, Ni, Ru and Pd), supported on metal oxides such as MnO, MgO, NiO, ZnO, CeO_2, La_2O_3, zeolites and carbon materials [6,14,15]. Homogeneous catalysts are usually more active for biomass depolymerisation and hydrolysis, but they are more challenging to recover from the reaction medium. On the contrary, heterogeneous catalysts are easier to recover but less active due to mass transfer (solid–solid) limitations occurring between the catalyst and the solid feedstock. Besides, they must be carefully synthesised to prevent their deactivation and/or decomposition under hydrothermal conditions [6]. Given these pros and cons, a sustainable alternative for the expansion and commercialisation of biorefinery processes is the use of autocatalytic reaction media. As HTTs use water as a reaction medium, seawater is an up-and-coming option to conduct hydrothermal reactions. It contains large amounts of dissolved species, such as chlorides, sulphides, and sodium, magnesium, calcium and potassium bi-carbonates, with catalytic activity during biomass depolymerisation [36,37]. Therefore, seawater might be an abundant, cheap and catalytic reaction medium for hydrothermal reactions, and a few works have addressed its possible use for the HTT of biomass. However, these have employed synthetic seawater [38] and the use of natural seawater for the HTT of biomass is infrequent [37] and unreported in the case of plastics.

Given this background, we hypothesise that different synergistic interactions between biomass and plastics affecting the yields and fuel and physicochemical properties of the reaction products can take place during the HTT of almond hulls and disposable face masks. Besides, seawater can also be a promising autocatalytic reaction medium for HTT due to the presence of dissolved species with catalytic activity. As a proof of concept, this work first-time addresses the synergetic co-valorisation of almond hulls (an unavoidable food waste) and FFP2 face masks (a common plastic material nowadays) using seawater at hydrothermal conditions (350 °C and 170 bar). The effects of the feedstock composition (each material alone and all possible binary combinations) and the reaction medium (deionised water, seawater and all possible binary mixtures) have been addressed over a wide range of reaction times (20–180 min). These analyses comprise the influence of these variables on the overall distribution of the reaction products (gas, biocrude, hydrochar and aqueous yield) and key fuel properties of the reaction products (chemical and elemental analyses and calorific values). The limited number of publications reporting on the use of seawater for the HTT of biomass and plastics, along with the intrinsic novelty of co-valorise both materials (almond hulls and FFP2 masks), demonstrate that this novel 'sea-thermal' approach represents a breakthrough for the development of future biorefineries, which contributes to reducing pollution, bringing out the hidden value of common residues from the human activity.

2. Experimental

2.1. Feedstocks and reaction medium characterisation

The almond hulls were from Marcona almonds harvested in Spain. They were first dried at 60 °C overnight to prevent mould formation during storage. Then, they were knife milled (Retsch ZM 200) and sieved to a particle size of c.a. 100–200 μm. The plastic residue comprises new FFP2 disposable face masks. After removing the nose wire and ear strap, these were cut into pieces (ca. 1 cm^2) manually and cryogenically milled (6770 Freezer/Mill) until fine powder (100–200 μm) was obtained. Almond hulls and disposable face masks were characterised by proximate and ultimate (elemental) analyses and fibre composition. Proximate and ultimate determinations were done according to ISO-18134:2016, ISO-18122:2016 and ISO-18123:2016, and the ash composition was determined by Inductively Coupled Plasma Optical Emission Spectrometry (ICP-OES) on a Spectroblue (AMETEK) apparatus. Lignocellulosic fibre composition (cellulose, hemicellulose and lignin contents) was determined by Van Soest titration [39], with the protein content being calculated using the N determined by elemental analysis [40]. Disposable face masks fibre analysis was determined following the experimental gravimetric methodology developed by Jung et al. [7]. The Fourier Transform Infrared (FT-IR) spectroscopy data, obtained on a Bruker Vertex 70 apparatus, are plotted in Figure S1. Table 1 shows the characterisation results, revealing that the data obtained align with those reported in the literature for almond hulls [41,42] and FFP2 face masks [7]. The ash composition of the almond hulls is provided in Table S1. Seawater, supplied by Rioka, was collected from the Matxitxako cape, at the Urdaibai biosphere reserve, in the Cantabrian sea (Spain). Deionised water and seawater were characterised by means of pH and conductivity (Crison MM1 analyser) and chemical composition. Anions were determined by Ionic Chromatography on a Methrom Series 800 Analyser, while cations were calculated by Inductive Couple Plasma Atomic Emission Spectroscopy (ICP-AES) on a Spectroblue-EOP-TI FMT26 analyser. The chemical properties of both types of water are listed in Table 2.

2.2. Hydrothermal treatment

The experiments were conducted in a 100 mL batch, pressurised autoclave (Parker Autoclave Engineers) made of stainless steel at 350 °C and 170 bar, using a solid/water ratio of 5 wt% and a stirrer rotation speed of 800 rpm. This solid/water ratio was selected to balance the energetic aspects of the process and their chemical singularities to ensure the prevalence of hydrothermal (low solid/water ratio) over thermal decomposition reactions (high solid/water ratio). Besides, the plastic material (disposable masks) is hygroscopic and solid loadings higher than 5 wt% resulted in a substantial material accumulation on the top of the reactor. The reactor vessel was heated by an external heating jacket, with the inner temperature being controlled by a PID controller and the total pressure monitored by a pressure gauge. A magnetic rotor (Magnedrive) controlled a stirrer bar used to homogenise the reaction medium, while a baffle and a coiled tube were employed to create a turbulent regime. Detailed information about the experimental bench can be found in our previous publications [22,43]. For each experiment, 50 mL of water (deionised water, seawater or a mixture of both) was loaded in the reactor with different amounts of solid material (almond hulls, disposable face masks or a binary mixture) according to the experimental design used in this work, using 2.5 g of solid material. Then, the reactor was purged with N_2 three times and filled in with N_2 until a final pressure of 30 bar was achieved at room temperature. Then, it was heated to achieve reaction conditions (350 °C, 170 bar). After

Table 1
Characterisation of almond hulls and FFP2 Face Masks.

Almond hulls		FFP2 Face Masks	
Proximate analysis (wt.%)			
Moisture	6.7 ± 2.9	Moisture	0.2 ± 0.1
Ash	11.8 ± 0.4	Ash	1.3 ± 0.6
Volatiles	62.7 ± 1.9	Volatiles	98.3 ± 0.1
Fixed carbon	18.8 ± 0.6	Fixed carbon	0.3 ± 0.4
Elemental analysis and HHV			
C (wt.%)	44.2 ± 1.4	C (wt.%)	84.0 ± 0.1
H (wt.%)	4.7 ± 0.2	H (wt.%)	13.3 ± 0.5
N (wt.%)	1.3 ± 0.1	N (wt.%)	0.0 ± 0.0
O[a] (wt.%)	49.9 ± 1.5	O[a] (wt.%)	2.8 ± 1.5
HHV (MJ/kg)	15.7 ± 0.5	HHV (MJ/kg)	44.7 ± 1.1
Fibre analysis (wt.%)			
Cellulose	12.6 ± 0.8	Polypropylene	69.5 ± 0.9
Hemicellulose	19.4 ± 1.2	Polyethylene	30.5 ± 0.9
Lignin	25.1 ± 2.5		
Proteins	7.8 ± 0.2		
Ash	11.8 ± 0.9		
Others	16.6 ± 1.3		

[a] O was calculated by difference.

Table 2
Characterisation of deionised water and seawater.

	Deionised water	Seawater
pH	6.43 ± 0.1	7.76 ± 0.1
Conductivity (mS/cm^2)	9.32 ± 0.47	50.08 ± 0.91
Anions (mg/L)		
Fl^-	<0.2	10
Cl^-	0.8	20,600
NO_3^-	0.3	10
SO_4^{2-}	<0.2	2900
Cations (mg/L)		
Ca^{2+}	<0.5	410
K^+	<0.5	458
Na^+	1.40	9988
Mg^{2+}	0.62	1232
S^{2+}	<0.5	897
Salinity[a] (ppm)	5	44,608

[a] Salinity was calculated as the total amount of ions.

each trial, the reactor was quenched to decrease the temperature to 50–60 °C as quickly as possible (ca. 15–20 min), and a gas aliquot was collected using a gas bag to analyse its composition. Subsequently, the reactor was opened, and the reaction products (liquid and solid fractions) were recovered. Additionally, the reactor vessel and the stirrer bar were rinsed with chloroform. Liquid and solid products were separated using a glass microfibre filter in a funnel. The solid fraction, namely hydrochar, was dried overnight at 105 °C and quantified gravimetrically. The liquid phase, comprising the biocrude and an aqueous liquid fraction, was subjected to a recovery process using chloroform and ethyl acetate as the solvents [44]. The aqueous phase was weighed for quantification, while the biocrude was subjected to a two-step solvent removal. First, both solvents (chloroform and ethyl acetate) were partially removed in a rotary evaporator. As a final step, a stream of pure N_2 was employed to obtain the solvent-free biocrude, which was weighed and stored for further analysis.

2.3. Analytical methodology and response variables

The yields to reaction products (gas, biocrude, hydrochar and aqueous phase) and some fundamental properties of these fractions were used as the response variables to study the influence of the feedstock mixture composition (almond hulls and disposable face masks), reaction medium (deionised water and seawater) and processing time (20–180 min) on the process. These include the chemical compositions of the gas and biocrude, along with the elemental compositions and calorific values of the gas, biocrude and hydrochar. Table 3 lists the response variables and summarises the methodologies employed for their calculation. A micro gas chromatograph (Micro-GC Varian CP4900) equipped with two packed columns (Molecular sieve and Porapack), coupled to a thermal conductivity detector (TCD), was used to analyse the gas. The gas yield was determined as the total amounts of H_2, CO, CO_2 and CH_4, assuming an ideal gas behaviour, and its LHV was estimated as the pondered heat of combustion of the mixture. The chemical composition of the biocrude was determined by gas chromatography-mass spectroscopy (GC–MS) on an Agilent 7890 GC-system. Elemental analyses of the biocrude and hydrochar were conducted using a Carlo Erba EA1108 Elemental Analyser, and their HHV were estimated with the empirical formula developed by Channiwala and Parikh [45]. The feedstock Energy Recovery (FER) gives an idea of the theoretical amount of energy efficiently transferred from the feedstock to the reaction products. This calculation does not consider some energetic singularities of the process, such as the process energy and heating losses.

2.4. Experimental plan and statistical tools

The influences on the process of the feedstock composition and reaction medium were addressed at 350 °C and 170 bar over a processing time varying between 20 and 180 min. These influences were calculated as the relative amount of disposable masks with respect to the total solid content (masks/masks + almond hulls) and the proportion of seawater with respect to the total water (seawater/seawater + deionised water), respectively. The experiments were planned following a two-level, three factor (2^3) Box-Wilson Central Composite Face Centred (CCF, α: ±1) design. This design includes 8 experiments (Runs 1–8) to analyse linear effects and interactions, 4 centre points (replicates) at intermediate conditions (Runs 9–12) and 6 axial experiments to determine quadratic influences and non-linear interactions (Runs 13–18). Such a methodology allows for studying the individual effects of each variable and detecting and quantifying interactions. The data were then analysed through a 95% confidence (p-value = 0.05) ANOVA (to determine significance) coupled with a cause-effect Pareto test (to calculate relative importance). For both tests, codec variables (between −1 and +1) were utilised, thus making the factors directly comparable. The codec formulae obtained from the ANOVA of the 18 runs were used to develop interaction plots showing the main effects and interactions detected. In addition, in these figures, some experimental points were added to show that the lack of fit is not significant graphically.

3. Results and discussion

Table 4 lists the experimental results obtained during the HTT at 350 °C and 170 bar of different almond hulls/disposable face masks mixtures using several water/seawater combinations. The full effects of the feedstock composition, reaction media and processing time on the experimental results according to the ANOVA and cause-effect Pareto Principle analyses are summarised in Table S2 (Supplementary Material).

3.1. Products distribution: gas, biocrude, aqueous fraction and hydrochar yields

The HHT of almond hulls and disposable masks leads to the formation of four main fractions, whose yields depend on the feedstock

Table 3
Response variables and methods.

Product	Response variable	Method
Gas	$\text{Gas yield}\,(\%) = \frac{\text{mass of gas}\,(g)}{\text{mass of feedstock}\,(g)}100$	Gas Chromatography
	$\text{Composition}\,(\text{vol.}\,\%) = \frac{\text{mol of each gas}}{\text{total mol of gas}}100$	Gas Chromatography
	$\text{LHV}\,(\text{MJ/m}^3\,\text{STP}) = 0.1079\,H_2\,(\text{vol.}\%) + 0.1263\,\text{CO}\,(\text{vol.}\%) + 0.3581\,CH_4\,(\text{vol.}\%)$	Estimated
	$\text{HHV}\,(\text{MJ/m}^3\,\text{STP}) = 0.1277\,H_2\,(\text{vol.}\%) + 0.1263\,\text{CO}\,(\text{vol.}\%) + 0.3990\,CH_4\,(\text{vol.}\%)$	Estimated
Biocrude	$\text{Biocrude yield}\,(\%) = \frac{\text{mass of biocrude}\,(g)}{\text{mass of feedstock}\,(g)}100$	Gravimetric
	$\text{C, H, O, N, S}\,(\text{wt.}\,\%) = \frac{\text{mass of C, H, O, N}\,(g)}{\text{mass of biocrude}\,(g)}100$	Elemental Analysis
	$\text{HHV}\,(\text{MJ/kg}) = 0.3491\text{C}\,(\text{wt.}\%) + 1.1783\text{H}\,(\text{wt.}\%) - 0.1034\text{O}\,(\text{wt.}\%) - 0.015\,\text{N}\,(\text{wt.}\%) + 0.1005\,\text{S}\,(\text{wt.}\%)$. [45]	Estimated
	$\text{Composition}\,(\text{Area}\,\%) = \frac{\textit{Area of each compound}}{\text{Total area of compounds}}100$	GC/MS
Liquid (aqueous)	$\text{Liquid yield}\,(\%) = \frac{\text{mass of liquid compounds}\,(g)}{\text{mass of feedstock}\,(g)}100 = 100 - (\text{Gas yield} + \text{Biocrude yield} + \text{Solid yield})$	Balance
Hydrochar	$\text{Solid yield}\,(\%) = \frac{\text{mass of hydrochar}\,(g)}{\text{mass of feedstock}\,(g)}100$	Gravimetric
	$\text{HHV}\,(\text{MJ/kg}) = 0.3491\text{C}\,(\text{wt.}\%) + 1.1783\text{H}\,(\text{wt.}\%) - 0.1034\text{O}\,(\text{wt.}\%) - 0.015\,\text{N}\,(\text{wt.}\%) + 0.1005\,\text{S}\,(\text{wt.}\%)$. [45]	Estimated
	$\text{C, H, O, N}\,(\text{wt.}\,\%) = \frac{\text{mass of C, H, O, N}\,(g)}{\text{mass of hydrochar}\,(g)}100$	Elemental Analysis
Feedstock Energy Recovery	$FER(\%) = \frac{\textit{Gas yield}\cdot\textit{HHV} + \textit{Biocrude yield}\cdot\textit{HHV} + \textit{Hydrochar yield}\cdot\textit{HHV}}{\textit{HHV of the feedstock mixture}}100$	Calculated

Table 4
Hydrothermal treatment experimental conditions: feedstock composition, medium composition and reaction time.

Run	1	2	3	4	5	6	7	8	9–12	13	14	15	16	17	18
M/M + A (wt.%)	0	100	0	100	0	100	0	100	50	0	100	50	50	50	50
S/S + D (wt.%)	0	0	100	100	0	0	100	100	50	50	50	0	100	50	50
t (min)	20	20	20	20	180	180	180	180	100	100	100	100	100	20	180
Overall products distribution															
Gas yield (%)	8.55	0.66	6.75	0.2	8.81	1.12	7.67	0.63	4.74 ± 0.21	11.99	0.27	4.44	4.27	4.75	4.77
Biocrude yield (%)	23.1	4.72	28.55	5.82	27.33	11.14	34.52	12.81	16.83 ± 0.60	23.91	4.11	18.96	17.31	15.42	16.63
Hydrochar yield (%)	16.2	78.69	30.53	82.11	14.23	85.77	28.65	86.53	49.97 ± 3.10	21.89	90.74	41.16	45.22	51.62	51.65
Aqueous yield (%)	52.14	15.94	34.17	11.86	49.63	1.98	29.15	0.03	28.46 ± 3.38	42.21	4.88	35.44	33.2	28.21	26.96
Gas composition and LHV															
H_2 (vol.%)	3.84	22.75	2.7	68.58	11.07	22.65	8.95	11.07	7.84 ± 0.75	4.88	62.49	8.18	9.52	4.73	11.55
CO_2 (vol.%)	77.92	36.61	86.3	31.42	77.49	41.45	79.84	77.49	76.89 ± 3.79	82.34	37.51	77.23	83.33	74.75	74.86
CO (vol.%)	13.63	0	9.4	0	9.87	5.97	9.5	9.87	12.82 ± 0.10	8.36	0	14.59	4.15	14.54	9.37
CH_4 (vol.%)	4.62	40.64	1.59	0	1.57	29.94	1.71	1.57	2.45 ± 3.25	4.42	0	0	3.00	5.98	4.22
LHV (MJ/m^3 STP)	3.79	17.01	2.05	7.4	3	13.92	2.78	3	3.34 ± 1.22	3.16	6.74	2.73	2.63	4.49	3.94
Hydrochar elemental composition and HHV															
C (wt.%)	66.8	85.6	47.8	85.6	70.7	85.3	47.8	84.5	84.38 ± 0.33	53.1	85.1	85.4	85.4	85	83.8
H (wt.%)	4.2	12.6	3.2	13.6	5	13.4	4.1	12.9	12.85 ± 0.34	3.4	12.3	13	13	12.9	12.8
O (wt.%)	26.6	1.7	44.5	0.7	22.2	1.2	46.6	2.4	2.65 ± 0.45	40.4	2.5	1.5	1.5	1.9	3.2
N (wt.%)	2.4	0.1	1.5	0.1	2.1	0.1	1.5	0.2	0.13 ± 0.05	1.6	0.1	0.1	0.1	0.2	0.2
HHV (MJ/Kg)	25.48	44.55	16.13	45.83	28.24	45.44	16.68	44.45	44.32 ± 0.45	18.49	43.94	44.97	44.97	44.67	44.01
Biocrude elemental composition and HHV															
C (wt.%)	71.5	60.9	63.8	56.7	70.2	61.8	67	74.3	69.80 ± 0.74	75.8	63.1	68.4	65.8	64	63.3
H (wt.%)	7.6	10.6	7.2	10	7.9	8.7	7.5	11.3	7.98 ± 0.17	9.1	9.2	7.8	7.5	8.1	7.7
O (wt.%)	19.1	28.1	27.3	32.8	19.9	28.4	23.5	14.1	20.58 ± 1.14	13.4	27.2	22.2	25.3	26.9	28
N (wt.%)	1.8	0.4	1.6	0.5	2	1.1	2	0.3	1.65 ± 0.25	1.7	0.5	1.6	1.4	1.0	1.0
HHV (MJ/Kg)	31.91	30.84	27.92	28.18	31.73	28.87	29.77	37.79	31.77 ± 0.48	35.77	30.05	30.75	29.17	29.09	28.26
Biocrude chemical composition (Area %)															
Ketones	45.02	0	45.36	0	35.2	0.49	35.87	0	16.61 ± 1.43	37.4	0.2	13.02	11.47	11.77	18.61
Phenols	37.88	16.91	22.2	28.9	40.64	7.25	43.09	5.57	33.80 ± 0.70	31.47	26	24.34	23.71	30.62	13.09
Cyclic alkanes	0	3.75	0	0	0	0.6	0	5.31	0.00 ± 0.00	0	0.17	0	0	0	0.83
Alkanes	0	26.49	0	10.67	2.24	2.26	0	20.84	0.00 ± 0.00	11.8	0.78	0.38	1.03	1.82	0
Alkenes	0	13.43	1.68	14.11	5.7	4.7	3.41	0.71	11.63 ± 1.40	9.01	7.01	9.04	8.51	16.01	13.67
Aromatic compounds	0	27.44	2.99	18.14	8.09	80.86	5.39	63.47	24.45 ± 0.70	1.03	65.19	32.67	43.15	13.47	44.47
Carboxylic acids	0	1.35	13.57	22.8	0	2.66	4.31	1.41	8.33 ± 0.84	0	0	11.46	8.51	15.76	3.69
Nitrogen compounds	17.1	1.96	14.21	0	8.14	0.58	7.93	0	5.19 ± 0.43	9.28	0.29	9.08	3.61	9.72	4.02
Alcohols	0	4.93	0	2.73	0	0	0	1.07	0.00 ± 0.00	0	0	0	0	0.82	0.83
Esters	0	3.74	0	2.64	0	1.07	0	5.13	0.00 ± 0.00	0	0.37	0	0	0	0.79
Aqueous phase properties (after the HTT experiments)															
Conductivity (μS/cm)	6.22	0.98	47.75	41.76	5.89	0.76	50.04	39.61	25.36 ± 1.60	27.35	21.46	3.75	41.03	26.28	25.81
pH	6.78	4.94	6.70	5.00	7.32	5.36	6.90	3.71	5.42 ± 0.08	6.55	5.28	5.95	5.85	5.27	5.47

composition, reaction medium and processing time, and vary as follows: gas (3–9%), biocrude (5–34%), hydrochar (13–87%) and aqueous fraction (0–54%). The cause-effect Pareto test reveals that the feedstock mixture exerts the most significant influence on the distribution of these products, with a relative importance higher than 65%. Regarding synergies between materials, the quadratic term in the models for the feedstock (F^2) is statistically significant in all the cases. This indicates the presence of synergistic or antagonistic effects between almond hulls and disposable face masks, which direct the overall distribution of the reaction products. These influences can be numerically assessed as the relationship between the quadratic terms and the total effects (linear and quadratic) of the feedstock ($F^2/F + F^2$) in the models. Such a calculation reveals synergies for the overall yields, whose importances are 15% for the gas, 33% for the biocrude, 8% for the hydrochar and 15% for the aqueous phase. These results are in line with the previous literature reporting on synergistic interactions between lignocellulosic biomass and plastic materials [27–30].

Besides, the reaction medium and processing time also impact the overall distribution of reaction products; yet, they have a less pronounced impact (e.g., 10% influence for the reaction medium). The quadratic term of the reaction medium (M^2) is significant, and its relative importance with respect to the total contribution ($M^2/M + M^2$) in the models is 75% for the gas yield, 47% for the biocrude yield and 39% for the hydrochar yield. These values indicate that the impact of seawater in the process is not linear, and it is necessary to have a minimum amount of seawater (>40 wt%) in the liquid medium to observe the promotional effects of seawater. On the contrary, the effect of the reaction medium is mostly linear for the liquid yield, with this term in the model being negative, thus denoting a negative contribution. This indicates that increasing the amount of seawater in the reaction medium decreases the formation of aqueous phase liquid products. Such a decrease can have a thermodynamic origin, as an increase in the amounts of salts in water decreases the solubility of some organic compounds, which can facilitate their transfer from the aqueous to the biocrude phase.

Apart from these single effects, different interactions between the feedstock composition, reaction media and processing time affect the distribution of the main reaction products. Fig. 1 shows the effects of the feedstock composition (almond hulls and face masks binary mixtures) and reaction media (deionised water and seawater) on the distribution

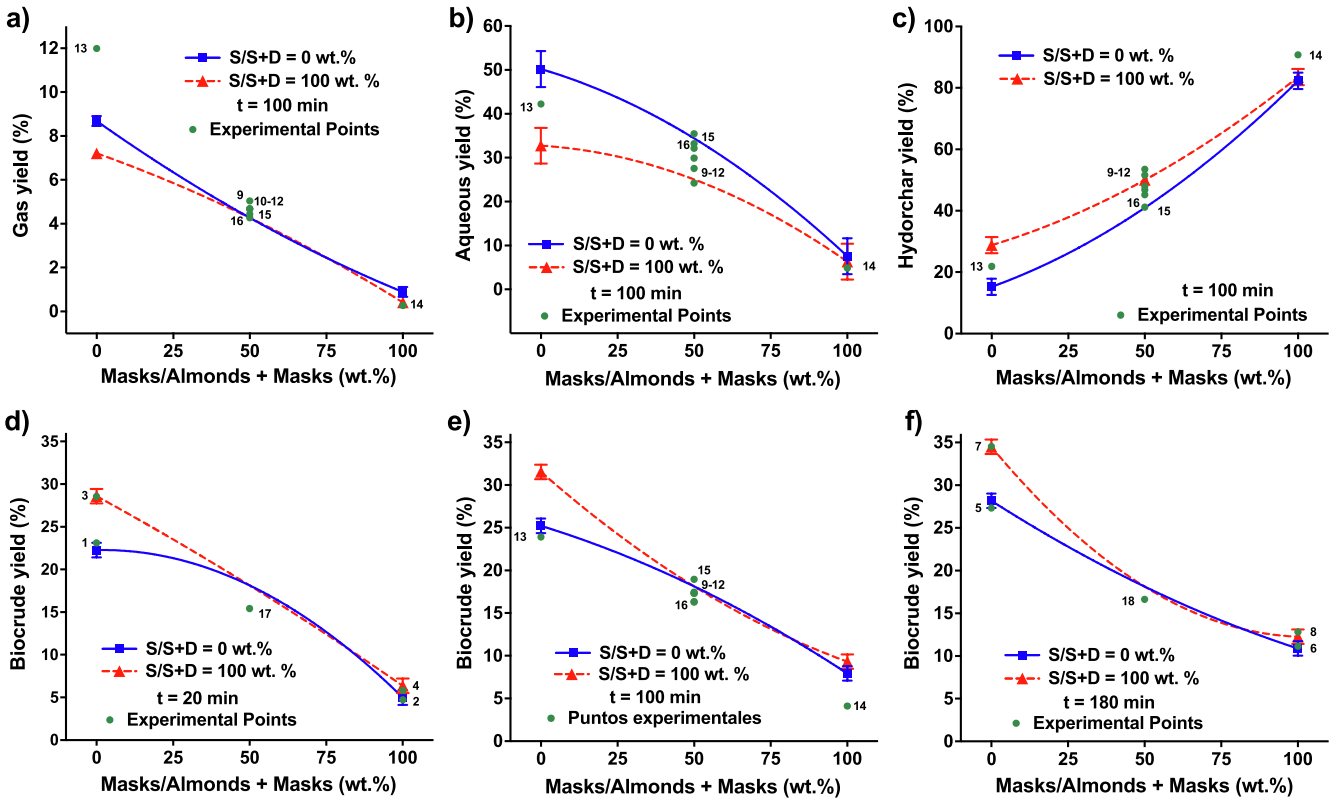

Fig. 1. Influence of the feedstock composition (disposable masks and almond hulls) using different water/seawater reaction media on the yields to gas (a), aqueous fraction (b) and hydrochar (c) at 100 min, and on the biocrude yield for a reaction time of 20 min (d), 100 min (e) and 180 min (f).

of the reaction products. The statistical analysis (Table S2) reveals that their impact does not depend on the reaction time for the gas, hydrochar and aqueous fraction yields. Thus, as an example, these effects are only plotted for an intermediate reaction time (100 min). Contrarily, the influences of the feedstock composition and reaction media on the biocrude yield depend on the reaction time, as denoted by the high importance of the interaction between the feedstock and reaction time (F^2t) term in the ANOVA and Pareto analyses (Table S2). Consequently, these influences have been assessed for short (20 min), intermediate (100 min) and long (180 min) reaction times.

Regardless of the reaction medium and processing time, the gas, aqueous fraction, hydrochar and biocrude yields depend on the feedstock mixture. When almond hulls are processed individually, higher gas, biocrude and aqueous yields and a lower hydrochar yield are obtained compared to those obtained with processing disposable face masks alone. These results are accounted for by the different structures of plastics in comparison with biomass [27]. In particular, the aliphatic plastics (polyethylene and polypropylene) in face masks are less prone to depolymerise due to the strength of the sp^3 C–C bonds present in their structures, which results in high solid production and low formations of gas, liquid and biocrude [26]. Consequently, the progressive addition of disposable masks to a feedstock comprising almond hulls leads to progressive decreases in the gas, biocrude and aqueous fraction production at the expense of hydrochar formation. These variations do not follow a linear trend, which indicates the existence of synergistic and antagonistic effects between almond hulls and disposable face masks, as described earlier. The aqueous fraction and biocrude (for short reaction times) display a convex pattern, while the gas and hydrochar yields have concave shapes. These developments indicate that the addition of disposable face masks contributes to liquefaction, increasing the formation of biocrude and aqueous products at the expense of the production of gas and hydrochar. The hydrothermal decomposition of almond hulls leads to the formation of active fragments [22]. These can act as active donors at the beginning of the polymer chain scissions occurring during the hydrothermal decomposition of polyethylene and polypropylene [30] in face masks. In parallel, the transfer of hydrogen from these polyolefinic chains helps stabilise the free radicals produced from the thermal decomposition of almond hulls, leading to higher biocrude and aqueous fraction productions and less gas and solid formation [30]. As a result, regardless of the reaction time, the variations observed in the gas, aqueous fraction and hydrochar yields with the addition of up to 50% of disposable face mask in the feedstock are less pronounced than those occurring with increasing the amount of this material from this point to a feedstock comprising face masks alone. This denotes that it is possible to co-process up to 50 wt% face masks with almond hulls without modifying these yields.

Increasing the reaction time from 20 to 180 min increases the gas and biocrude yield at the expense of the hydrochar yield, with the aqueous fraction yield unaffected. Besides, the influence of the feedstock depends on the reaction time for the biocrude yield, and further developments occur depending on the reaction time. When a short reaction time (20 min) is used, a convex decrease is observed, which produces a trade-off in the biocrude yield with increasing the proportion of masks in the mixture from 0 to 50 wt%. An increase in the reaction time up to 100 min increases the biocrude yield for pure almond hulls and enriched mixtures, which modifies the shape of the curve towards a convex decay. The biocrude yields for almond hulls and enriched mixtures increase with prolonging the processing time up to 180 min. These results indicate that the free radical stabilisation, hampering the formation of gas and hydrochar, occurs at the early reaction stages. Thus, using long reaction times limits the positive effect of hydrogen transfer reactions, leading to an antagonistic biocrude production. This leads to a convex evolution in the biocrude yield with increasing the proportion of face masks in the feedstock. As a result, the trade-off observed in the biocrude yield shifts towards enriched in masks (>60 wt%) mixtures.

The reaction medium also exerts a significant influence on the

distribution of the overall reaction products, and its impact depends on the feedstock. On the one hand, when almond hulls are processed alone, augmenting the relative amount of seawater in the medium decreases the gas and aqueous yields, leading to increments in the biocrude and hydrochar yields. These results indicate that seawater positively influences biomass depolymerisation, favouring biocrude production. Jiang et al. [36] reported that NaCl was the main responsible for the positive effect of seawater in biomass depolymerisation. In particular, Cl^- species disrupted the hydrogen bonding network of biomass derived-structures, favouring depolymerisation via scission of O–H bonds. In another work, Yang et al. [38] reported that the activation energy for H dissociation in hydroxyl groups (–OH) was three times lower in seawater than in deionised water. Additionally, Ding et al. [46] and Jena et al. [47] also reported that Na_2CO_3 increased the biocrude yield during the hydrothermal liquefaction of biomass. On the other hand, the reaction medium does not significantly influence these yields using disposable masks as a feedstock, and the effect of seawater decreases progressively with increasing the proportion of disposable masks. As a result, the same yields are obtained with deionised water or seawater during the HTT of face masks, which suggests that seawater does not catalyse the C–C scissions needed for polypropylene and polyethylene depolymerisation under the operating conditions used in this work.

While the same evolutions as described for deionised water occurs in seawater for the gas, aqueous and hydrochar yields, the influence of the feedstock mixture and reaction time on the biocrude yield is altered, with different outcomes taking place depending on the reaction medium. When the process is conducted in deionised water, the biocrude yield decreases convexly, as described above. Conversely, increasing the amount of seawater modifies the effect of the feedstock from a concave to a convex decay for reaction times longer than 100 min. As a result, when the process is conducted for 180 min, disposable face masks exert an antagonistic effect of biocrude production using long reaction times. NaCl has also been reported to favour biocrude conversion into gases via thermal cracking and solid products by repolymerisation [37,38], with these transformations occurring to a more significant extent with prolonging the processing time.

3.2. Composition and LHV of the gas phase

The gas phase comprises H_2 (3–69 vol%), CO_2 (31–86 vol%), CO (0–15 vol%) and CH_4 (0–34 vol%), with its LHV ranging from 1 to 17 MJ/m^3 STP. The statistical analysis reveals that the proportions of H_2, CO_2 and CO in the gas and its LHV principally depend on the feedstock, while the reaction medium and processing time determine the concentration of CH_4. The relationships between the contribution of quadratic effects with respect to the total feedstock effects ($F^2/F + F^2$) for the properties of the gas reveal important synergies (40% for H_2, 33% for CO_2, 56% for CO and 36% for CH_4) and the LHV (39%). Besides, the reaction medium also impacts the properties of the gas phase significantly, with an important contribution of the quadratic effect respecting the total contribution (37% for H_2, 22% for CO_2, 30% for CO and 31% for CH_4 volumetric compositions and 15% for the LHV). The reaction time exerts a substantial effect on the gas phase properties and modifies the influences of the feedstock and reaction medium. Fig. 2 shows the effects of the feedstock and reaction medium on the chemical composition and LHV of the gas phase. Fig. 2 a/e/h/k/n shows the influence of the feedstock mixture on the proportions of $H_2/CO_2/CO/CH_4$ and LHV with a reaction medium comprising deionised water and seawater, using a reaction time of 20 min. These effects are plotted in Fig. 2 b/f/i/l/o and Fig. 2 d/g/j/m/p for a reaction time of 100 and 180 min, respectively.

The influence of the feedstock mixture depends on the reaction medium and processing time. When the process is conducted with deionised water for a short reaction time (20 min), the gas phase comprises mainly CO_2 and CO, leading to a gaseous product with a meagre LHV. This is in line with the literature reporting on the HTT of biomass. At high temperatures (>300 °C), decarboxylation via pyrolysis, thermal decomposition and cracking occur to a significant extent, leading to a gas fraction primarily comprising CO_2 [11,16,48]. The progressive addition of face masks to the solid mixture gradually decreases the relative amounts of CO_2 and CO at the expense of the proportions of H_2 and CH_4 due to the lower O/C and higher H/C ratio of face masks compared to those of almond hulls. However, such developments do not follow a linear pattern, denoting interactions between both materials affecting the gas phase composition. Notably, increasing the proportions of face masks in the feedstock mixture up to 50 wt% does not substantially modify the chemical composition of the gas. Only a slight decrease is observed for the proportion of CO in the gas phase, which is compensated by an increase in the relative amount of CO_2. On the contrary, sharp variations are observed when the proportion of face masks increased from 50 wt% to a feedstock consisting of face masks only. For this reaction medium (deionised water), the effect of the reaction time primarily depends on the feedstock. These variations are accounted for by the convex patterns in the proportions of CO_2 and CO, denoting a feedstock synergistic influence, and the concave evolutions of the proportion of H_2 and CH_4, showing a feedstock antagonistic effect. These might be caused by the consumption of H species released from the polyolefinic chains in face masks during the stabilisation of the free radical produced from the thermal decomposition of almond hulls. As a result, the gas contains more significant amounts of CO_2 and CO and lower proportions of H_2 and CH_4 than those theoretically expected taking into account the cumulative production of each feedstock in the mixture without interactions.

When almond hulls are processed alone, increasing the reaction time progressively upsurges the amount of H_2 in the gas at the expense of the relative amount of CO, as increasing the processing time can shift the water gas shift reaction ($CO + H_2O \Leftrightarrow CO_2 + H_2$) towards H_2 production [22,49,50]. However, increasing the proportion of disposable face masks in the feedstock progressively modifies the effect of the reaction time. The same increase in time leads to increases in the proportion of H_2 at the expense of the relative amounts of CO_2 and CO when an equimassic mixture is processed. Conversely, for pure face masks, lengthening the reaction time does not substantially affect the gas composition; only small diminishments in the proportions of H_2 and CO occur, accompanied by a minimal increase in the concentration of CH_4. These minor variations are believed to account for the low gas production achieved when face masks are used as the feedstock. As a result of these developments, the LHV of the gas remains low when almond hulls are processed and increases sharply with a proportion of face masks higher than 50 wt%. The effect of the reaction time on the gas LHV is only significant for face masks enriched mixtures, with decreases occurring when the reaction time increases from 20 to 180 min. However, these variations are not important from a practical point of view due to the low energetic value of the gas phase (14–16 MJ/m^3 STP) and the small amount of gas produced.

The effect of the reaction medium depends on the feedstock and reaction time. For a feedstock consisting of pure almond hulls, similar gas compositions are obtained regardless of the reaction time and type of water used. This is in line with the minimal effect exerted by the seawater on gas production, as described earlier. Conversely, increasing the proportion of face masks in the solid feedstock modifies the influence of the reaction medium, with different evolutions depending on the processing time. For a short reaction time (20 min), enriching the reaction mixture in seawater increases the proportion of H_2 in the gas at the expense of the proportions of CO and CH_4. While minor variations are observed for a feedstock comprising up to 50 wt% of face masks, the proportion of H_2 increases and the relative amount of CH_4 decreases very sharply for a feedstock containing more than 50 wt% face masks. This suggests that seawater promotes a more significant development of the methane reforming reaction ($CH_4 + H_2O \Leftrightarrow CO + 3H_2$) due to the presence of alkali salts, which exerts a catalytic influence during the HTT of biomass [9,51,52]. A progressive increase in the reaction time

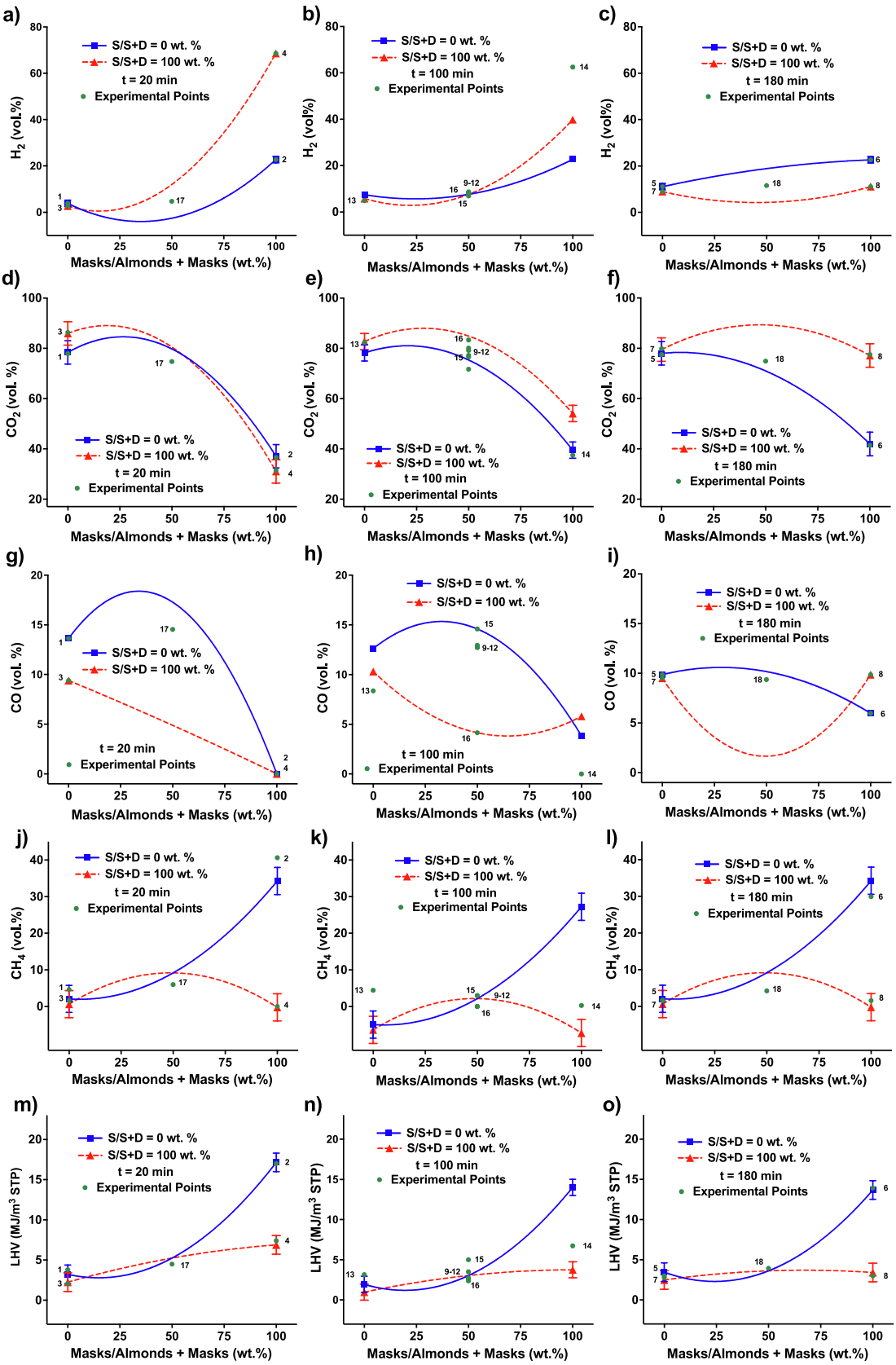

Fig. 2. Influence of the feedstock composition (disposable masks and almond hulls) using different water/seawater reaction media on the proportions of H_2 (a-c) CO_2 (d-f), CO (g-i) and CH_4 (j-l) and LHV (m-o) of the gas using a processing time of 20, 100 and 180 min.

from 20 to 180 min decreases the differences in the proportions of H_2 and CO_2 obtained with deionised water and seawater. This is accounted for by the significant influence of the reaction time during the processing of face masks in seawater, which can disguise the positive catalytic effect of alkali salts in seawater. In this case, increasing the reaction time leads to a substantial decrease in the concentration of H_2 at the expense of the relative amount of CO_2 in the gas when the process is conducted with seawater. As a result of these variations, the feedstock does not substantially influence the volumetric composition of the gas phase, and similar gas compositions are obtained by coprocessing almond hulls and/or face masks in seawater for 180 min. Regardless of the reaction time, the gas LHV decreases in the presence of seawater when the feedstock contains more than 50 wt% face masks due to the diminishments occurring in the proportions of H_2 and CH_4.

3.3. Hydrochar elemental composition and HHV

The solid product obtained during the HTT of almond hulls and disposable face masks (alone or in combination) resembles a hydrochar-like material. The elemental composition of this solid varies by 48–86 wt % C, 3–14 wt% H, 1–46 wt% O, 0–2 wt% N, which shifts its HVV between 16 and 46 MJ/kg. The variation interval for the relative amount of C is in line with the C content of almond hulls (44 wt%) and disposable face masks (84 wt%). The statistical analysis reveals that the elemental composition and HHV of the hydrochar are primarily affected by the feedstock composition (influence greater than 60% in all the cases). Second in importance is the feedstock-reaction medium interaction term (FM and F^2M), which indicates that the effect of the feedstock is substantially affected by the reaction medium. Synergistic and antagonistic effects between almond hulls and disposable face masks affecting the properties of the hydrochar also take place due to the significant influence of the quadratic term of the feedstock (F^2) in the models. The relationship between quadratic and total terms for the feedstock ($F^2/F^2 + F$) shows that the impact of the synergistic and/or antagonistic effects is around 40% for the elemental composition and HHV of the hydrochar. This analysis reveals that the reaction time does not significantly influence the hydrochar properties. As an example, Fig. 3 plots the influence of the feedstock on the elemental composition and HHV of the hydrochar using different deionised water/seawater combinations for an intermediate processing time (100 min).

Regardless of the reaction medium or processing time, the hydrochar produced from almond hulls contains less C and H and more O and N than that obtained during the hydrothermal treatment of disposable face masks. As a result, the HHV of the hydrochar obtained from the former feedstock is lower than that from the latter. These results account for the greater O and N and lower H and C contents in almond hulls compared to those in disposable face masks. Given these differences, increasing the proportion of face masks in the feedstock progressively increases the proportions of C and H and lowers the relative amounts of O and N of the hydrochar, leading to a substantial increase in the HHV of this product. These evolutions do not follow a linear trend, which denotes the existence of significant interactions between materials affecting the elemental composition and HHV of the hydrochar. On the one hand, the increases in the proportion of C and H and HHV follow convex trends, denoting a synergistic impact. On the other, the relative amounts of O and N decrease concavely, indicating a feedstock antagonistic effect. Such interactions indicate a more significant extension of deoxygenation, decarboxylation, dehydration, condensation, cyclisation, deamination and thermal cracking transformations [16,53] for the binary mixtures than those theoretically expected, taking into consideration the individual contribution of each feedstock. Such developments can result from the presence in the reaction medium of H species released from plastic materials. Several authors have reported that polyethylene and polypropylene can act as a hydrogen source for biomass liquefaction,

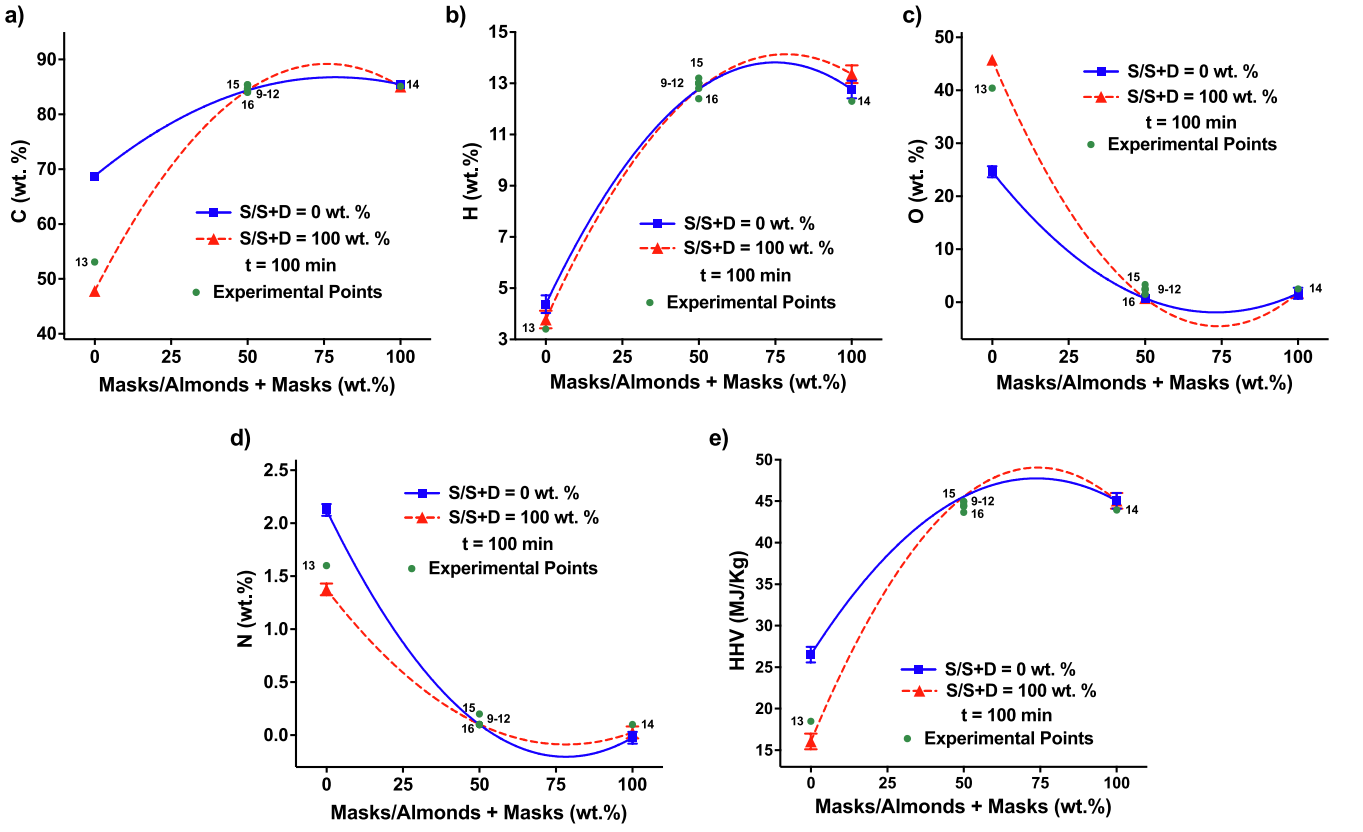

Fig. 3. Influence of the feedstock composition (disposable masks and almond hulls) using different water/seawater reaction media on the proportions of C (a), H (b), O (c) and N (d) and the HHV (e) of the hydrochar using a processing time of 100 min.

enhancing the fuel properties of the biocrude and hydrochar [31,32]. These developments also decrease the H/C and O/H ratios, which have been assumed to account for a greater degree of aromaticity and stability [6]. In addition, these variations are markedly significant when the proportion of disposable face masks in the feedstock varies from a feedstock comprising pure almond hulls to an equimassic almond hulls/disposable face masks mixture. A further increase in the proportion of disposable masks does not modify the elemental composition or HHV of

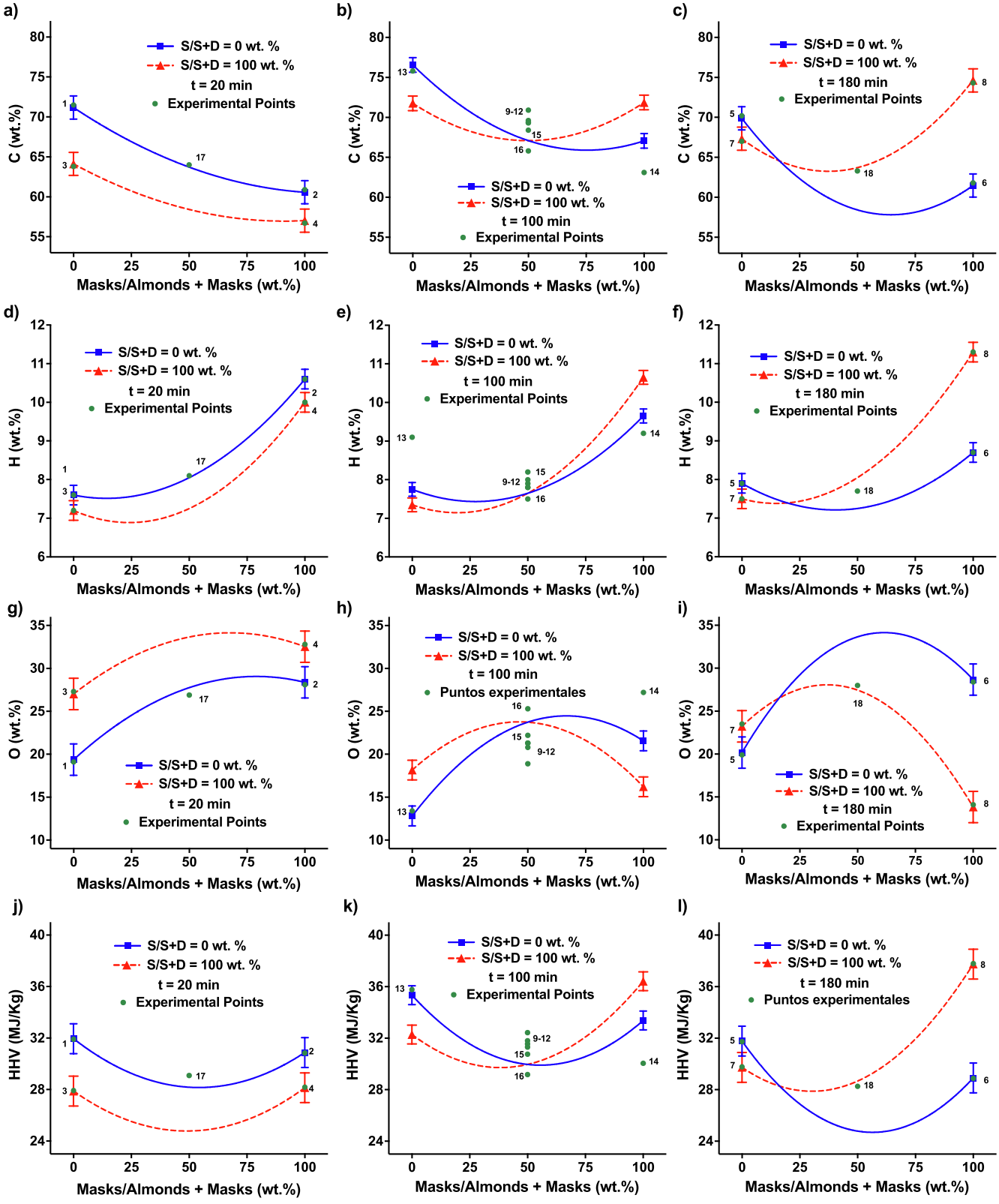

Fig. 4. Influence of the feedstock composition (disposable masks and almond hulls) using different water/seawater reaction media on the relative amounts of C (a-c), H (d-f), O (g-i) and HHV (j-l) of the biocrude using a processing time of 20, 100 and 180 min.

the hydrochar, and similar values are obtained coprocessing these binary mixtures than processing disposable face masks alone.

The effect of the reaction medium depends on the feedstock. In particular, an increase in the proportion of seawater decreases the proportions of C and N at the expense of the relative amount of O without modifying the proportion of H in the hydrochar. These variations lead to a decrease in the HHV of the hydrochar. As the proportion of face masks in the feedstock mixture increases, these variations are less marked. As a result, the effect of the reaction medium is not significant for feedstock mixtures comprising more than 50 wt% disposable masks. These results might be accounted for by the positive catalytic influence of alkali salts in seawater on repolymerisation and condensation [38], thus increasing the proportion of O and diminishing the relative amount of C in the hydrochar.

3.4. Biocrude elemental composition and HHV

The elemental composition of the biocrude varies by 57–77 wt% C, 7–11 wt% H, 13–33 wt% O and 0–2 wt% N, which shifts the HHV of this product between 28 and 38 MJ/kg. The statistical analysis of these data reveals that the feedstock is the variable exerting the most influential effect on the elemental composition and HHV of the biocrude. Interactions between materials affecting these variables are statistically significant due to the significant influence of the quadratic term for the feedstock composition in the ANOVA analyses. The quadratic contribution of the feedstock with respect to total effects is around 30% for the elemental composition and 40% for the HHV of the biocrude. On the contrary, the individual effects of the processing time and reaction medium are less critical. Nevertheless, these variables alter the individual effect of the feedstock due to the substantial number of interactions between the feedstock and processing time and reaction medium. Fig. 4 a-c/d-f/g-i/j-l plots the influence of the feedstock composition on the relative amount of C/H/O and HHV of the biocrude for different reaction media (water/seawater) when the treatment is conducted for 20, 100 and 180 min.

When the valorisation process is conducted in deionised water, the biocrude produced from almond hulls contains a higher proportion of C and lower H and O relative contents than those obtained from disposable face masks, regardless of the processing time. These results are accounted for by the lower biocrude yield produced with disposable face masks and the fact that part of the O of the reaction medium (H_2O) can be incorporated into the biocrude [26]. Mainly, polypropylene and polyethylene contain aliphatic carbon atoms leading to the formation of intermediate species in the biocrude capable of reacting with H_2O [26]. In this regard, the little biocrude produced with face masks makes it possible that this fraction has a relative high O content even though the total O content is low. The progressive incorporation of face masks into a feedstock comprising almond hulls leads to a decrease in the proportion of C at the expense of the relative amounts of H and O, with these variations not following linear trends. This denotes antagonistic interactions (concave evolutions) for the proportions of C and H and synergistic interactions for the relative amount of O (convex evolution). As a result, a biocrude with greater O and lower C and H contents and HHV is produced compared to that expected from the individual contribution of each feedstock. These variations are in line with the increases occurring for the biocrude yield. A reactive hydrogen atmosphere produced via the presence of H reactive species from polypropylene and polystyrene decomposition increases the biocrude formation as described earlier [30]. It also helps biocrude stabilisation, thus avoiding the deoxygenation of this product via possible cracking and reforming reactions [43]. Consequently, the relative amount of H displays a trade-off with increasing the proportion of plastic masks in a feedstock comprising pure almond hulls, until an equimassic mixture is achieved. In these cases, the decreases in the proportion of C account for increases in the relative amount of O in the biocrude. A further increase in the proportion of face masks in the feedstock mixture above 50 wt% does not modify the amount of O in the biocrude, and less pronounced decreases in the proportion of O take place, with these being compensated by small increments in the relative amount of H.

Using deionised water as a reaction medium, the processing time primarily influences the proportions of C and O in the biocrude, with the variations occurring in the H content being insignificant from a practical point of view. In particular, prolonging the processing time from 20 to 100 min time leads to an initial increase in the concentration of C in the biocrude at the expense of the relative amount of O, regardless of the feedstock composition, leading to increases in the HHV of the biocrude. Such variations account for the beneficial kinetic impact of the reaction time on the process, which produced a greater spread of deoxygenation, deamination and thermal cracking reactions [54–57]. However, a subsequent time increment to 180 min diminishes the proportion of C and upsurges the relative amount of O of this product, diminishing the biocrude HHV. Using long processing times promotes biocrude transformation into gaseous products via reforming, pyrolysis and/or thermal cracking. As a consequence, light oxygenates in the biocrude can be removed, which might result in a product with a high oxygen content [22]. On the contrary, the impact of the reaction time on the relative amount of H in the biocrude depends on the feedstock.

The influence of replacing deionised water with seawater depends on the processing time. For a short reaction time (20 min), augmenting the proportion of seawater decreases the amounts of C and H in the biocrude and upsurges the proportion of O, regardless of the feedstock composition. Such variations lead to a decrease in the HHV of this fraction. For pure almond hulls and enriched mixtures, these results are the consequence of different kinetic and thermodynamic influences of seawater on the process. On the one hand, such a positive kinetic influence not only increases the biocrude production, as described earlier, but also promotes the decomposition of some light oxygenates in the biocrude [22]. On the other, increasing the amounts of salts in water decreases the solubility of some organic compounds, which can facilitate their transfer from the aqueous to the biocrude phase, which increases the biocrude yield and its O content. For pure face masks, such variations indicate that salts might inhibit the incorporation of O from water to the biocrude and/or favour its subsequent removal.

When the process is conducted with seawater, an increase in the reaction time from 20 to 100 min leads to a substantial increase in the relative amount of C, dropping the proportion of O without modifying the H content of the biocrude. These variations are a consequence of the positive kinetic impact of the reaction on the process, which produced a greater spread of deoxygenation and thermal cracking reactions [54–57]. As a result, for 100 min processing time, the effect of the reaction medium depends on the feedstock composition, with two development occurring. On the one side, when pure almond hulls or mixtures containing up to 50 wt% almond hulls are processed, the proportions of C and H decrease at the expense of the relative amount of O when deionised water is progressively substituted by seawater. These variations are accounted for by the different thermodynamic and kinetic effects exerted by seawater as described above. On the other, this progressive incorporation of seawater leads to increases in the relative amounts of C and H and a diminishment in the proportion of O when the feedstock contains more than 50 wt% face masks, as the transfer of oxygenates from the aqueous phase to the biocrude fraction occurs to a lesser extent due to the decrease occurring in the aqueous fraction yield with increasing the amount of disposable face masks in the feedstock. A subsequent time enlargement from 100 to 180 min using seawater affects the biocrude elemental composition when the feedstock contains a high proportion (>50 wt%) of face masks. Thus, when a long (180 min) processing time is used, the effect of the reaction medium is at its greatest when the feedstock contains more than 50 wt% of disposable masks. In such cases, the progressive substitution of deionised water by seawater increases the proportions of C and H and decreases the relative amount of O in the biocrude, with the variations being substantially more marked with augmenting the proportion of face masks in the

feedstock. An increase in the amount of seawater promotes the deoxygenation of the biocrude produced from disposable face masks, with this process being favoured using a long reaction time. Therefore, these results indicate that the decrease in the O content of the biocrude produced from face masks promoted by seawater occurs via O elimination rather than O inclusion inhibition.

3.5. Biocrude chemical composition

The biocrude consists of a pool of different chemicals, including oxygenate, aliphatic, aromatic and nitrogen-containing compounds (Table S3). These include phenols (5–51%), ketones (0–45%), aromatic compounds (0–81%), carboxylic acids (0–23%), nitrogen-containing compounds (0–17%), alkanes (0–26), alkenes (0–15%) and cyclic alkanes (0–5%). The statistical analysis reveals that the chemical composition of the biocrude primarily depends on the feedstock and reaction medium, with the processing time playing a less influential role. The relationships between the contribution of quadratic effects with respect to the total feedstock contribution ($F^2/F + F^2$) for the biocrude chemical composition reveal important synergies (c.a., 10% for nitrogen-containing compounds, 20–25% for ketones, phenols and aromatic compounds and 35–40% for alkanes, alkenes and cyclic alkanes). Besides, the quadratic contribution is also important for the majority of these species, denoting that the influence of the reaction medium is not linear and a minimum amount of seawater is needed to alter the effects of deionised water. Fig. 5a-c/d-f/g-i/j-l/m-o/p-r plots the influence of the feedstock composition on the relative amounts of the most abundant species (phenols, ketones, aromatic compounds, carboxylic acids, nitrogen compounds, alkanes and alkenes) in the biocrude for different reaction media (water/seawater) when the treatment is conducted for 20, 100 and 180 min.

The effect of the feedstock mixture on the biocrude chemical composition depends on the reaction medium and processing time. When the process is conducted using deionised water, the biocrude produced with almond hulls is principally made up of phenols, ketones, and nitrogen-containing species regardless of the processing time. At the same time, aromatic compounds, alkanes and alkenes constitute the biocrude when disposable face masks are used as a feedstock as polypropylene and polyethylene alkyl structures lead to liquid products resulting from C-C bond cleavages [26]. These results align with the chemical composition of biocrudes produced from lignocellulosic biomass and plastic materials [5,15,26,30,58]. The evolution of these species when the feedstock transitions from a pure to a binary mixture is not linear, denoting significant interactions between materials. A first progressive addition of up to 50–60 wt% disposable masks to a feedstock containing pure almond hulls leads to concave decreases in the proportions of phenols and ketones and a convex decrease in the proportion of nitrogen-containing compounds at the expense of convex increases in the relative amounts of aromatic compounds, carboxylic acids and alkenes. A subsequent increment in the amount of face masks in the feedstock significantly increases the proportions of aromatic compounds and alkenes, diminishing the proportion of carboxylic acids without substantially affecting the proportions of phenols or ketones. Aromatisation and condensation reactions [38], upsurging the relative amount of aromatic compounds, might be responsible for such variations.

Besides, the shapes of these curves denote synergistic increases in the proportions of aromatic compounds, carboxylic acids, nitrogen-containing species and alkenes at the expense of antagonistic diminishments in the relative amounts of phenols, ketones and alkanes co-feeding materials in comparison with the compositions expected considering the individual contribution of each material. Previous work reporting on the promoting effect of plastic materials in the decomposition of lignocellulosic biomass helps explain these developments.

For example, plastic materials promote the formation of alkyl compounds from the decomposition of triglycerides in lignocellulosic biomass [27], which might account for the synergistic increment in the proportion of alkenes in this work. These plastics also activate protein decomposition, which leads to increases in the proportion of proteins in the biocrude [6] and helps stabilise the intermediates produced from lignocellulosic biomass dehydration, boosting the formation of aromatic compounds [5]. Consequently, these synergistic increments produce diminishments in the proportions of phenols and ketones. These latter chemicals can be converted to N-containing species in the presence of NH_3 [58], which can result from the plastic-promoted decomposition of proteins of lignocellulosic biomass. Additionally, Seshasayee et al. reported that polyolefins antagonistically decreased the proportion of phenols in the biocrude at the expense of aromatics formation [5].

Although similar evolutions occur regardless of the reaction time,

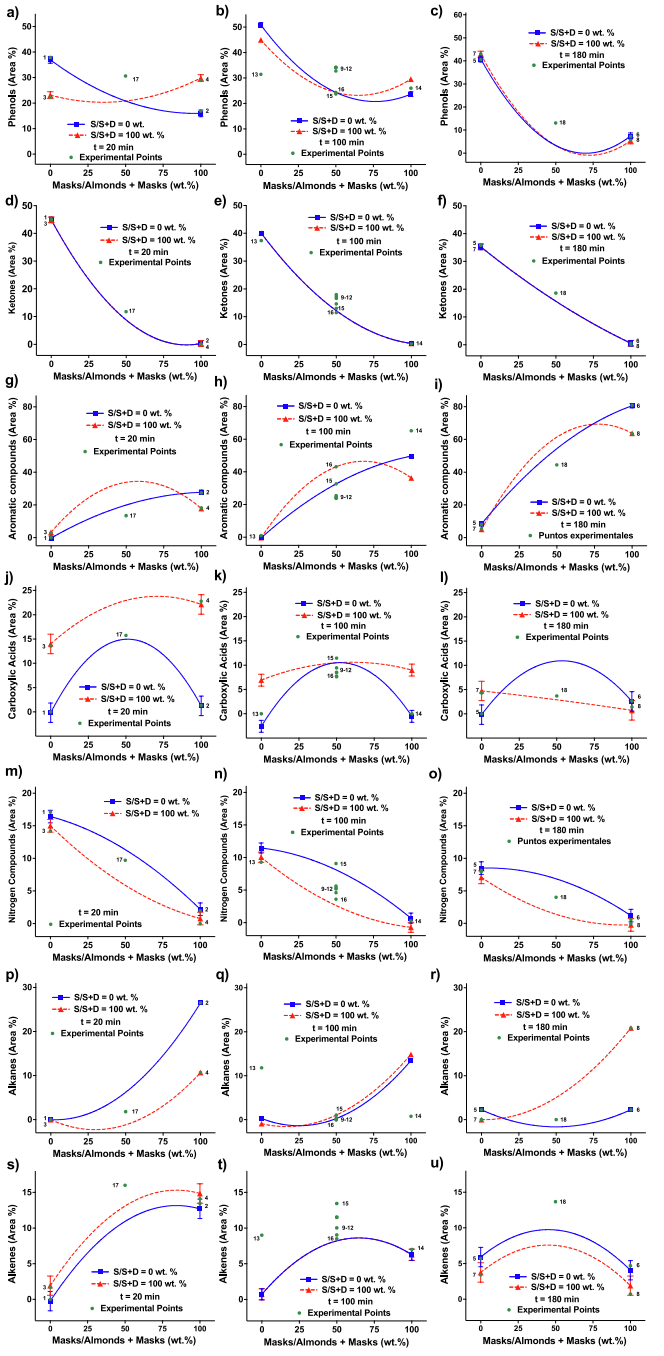

Fig. 5. Influence of the feedstock composition using different reaction media on the relative amounts of phenols (a-c), ketones (d-f), aromatic compounds (g-i), carboxylic acids (j-l), nitrogen compounds (m-o), alkanes (p-r) and alkenes (s-u) in the biocrude using a processing time of 20, 100 and 180 min.

effect of this variable relay on the feedstock composition (Fig. 5 a/d/g/j/m/p/s/ vs b/e/h/k/n/q/t vs c/f/i/l/o/r/u). For pure almond hulls, the effect of the reaction time is meagre, and only minimal increases occur in the proportion of phenols, along with slight decreases in the relative amounts of ketones and nitrogen-containing compounds. However, these variations are not important from a practical point of view. On the contrary, the effect of the reaction time is more important when mixtures comprising >50 wt% face masks are used as the feedstock. In these cases, increasing the reaction time decreases the proportions of phenols, alkanes and alkenes at the expense of a substantial increase in the relative amounts of aromatic compounds. These results are believed to be a consequence of the promoting effect of the processing time on polymerisation and condensation reactions [14–16,59], leading to the formation of aromatic macromolecules. Besides, the reaction time promotes the initial formation of reactive radicals by the homolytic rupture of sp^3 C–C bonds and their subsequent recombination and dehydrogenation along with more significant developments of Diels-Alder reactions [26].

Replacing deionised water with seawater does not lead to substantial changes in the chemical composition of the biocrude. The alterations observed depend on the feedstock composition and processing time. When a short reaction time (20 min) is used, the progressive substitution of deionised water with seawater increases the proportions of aromatic compounds and carboxylic acids and drops the relative amounts of nitrogen-containing species and alkanes. These developments can be accounted for by the promoting effect of seawater on condensation reactions [38], leading to increases in the relative amount of aromatic compounds. Besides, NaCl in seawater can also inhibit the development of Maillard reactions [37,38], which decreases the formation of nitrogen-containing species in the biocrude. As a result of these features, the effect of the feedstock mixture on the chemical composition of the biocrude differs from that described for deionised water. Using seawater, the progressive incorporation of face masks to a mixture comprising almond hulls in seawater leads to concave increases in aromatic compounds, carboxylic acids and alkenes coupled with a convex increase in the proportion of alkenes and convex decreases in the proportion of ketones and nitrogen-containing species. These variations are a consequence of the effects of seawater on promoting condensations and inhibiting Millard reactions [37,38], as described above. For a long reaction time (180 min), the progressive substitution of deionised water with seawater increases the proportion of alkenes at the expense of the relative amounts of carboxylic acids and aromatic compounds. Such a development suggests a positive kinetic influence on polyethylene and polypropylene depolymerisation when long reaction times are used. This agrees with the increase observed in the biocrude yield, increasing the reaction time during the HHT of disposable face masks in seawater, as described earlier.

3.6. Theoretical process optimisation

Six optimisation scenarios have been addressed to transform almond hulls and disposable face masks into liquid and solid biofuels utilising the formulae developed from the ANOVA of the experimental data (Table 5). The actual, adjusted and predicted regression (R^2, R^2_{adj} and R^2_{pred}) coefficients are greater than 0.95, the signal/noise ratios are higher than 4, and the lack of fit is not significant (p-value > 0.05) with

Table 5
Theoretical optimisation: objectives and optima for biofuels production.

Optimisation	1		2		3		4		5		6	
	Obj.	Sol.	Obj.	Sol.	Obj.	Sol	Obj.	Sol.	Obj.	Sol.	Obj.	Sol.
M/A + M (wt.%)		0	+(2)	20		92	-(2)	73		100	-(2)	78
S/S + D (wt.%)		0		5		84		95		100		100
t (min)		115		95		180		180		180		147
Overall product distribution												
Gas yield (%)		8.72 ± 0.20		7.23 ± 0.20		1.12 ± 0.20		2.82 ± 0.20		0.62 ± 0.20		2.39 ± 0.20
Biocrude yield (%)	+(3)	25.77 ± 0.79	+(3)	22.33 ± 0.79		10.40 ± 0.79		13.71 ± 0.79	+(3)	12.26 ± 0.79	+(3)	13.15 ± 0.79
Hydrochar yield (%)		14.90 ± 2.45		24.91 ± 2.45	+(3)	82.90 ± 2.45	+(3)	64.74 ± 2.45	+(3)	85.45 ± 2.45	+(3)	66.93 ± 2.45
Liquid yield (%)		49.54 ± 4.02		44.64 ± 4.02		6.99 ± 4.02		14.59 ± 4.02		2.86 ± 4.02		13.78 ± 4.02
Hydrochar elemental analysis and calorific value												
C (wt.%)		69.11 ± 0.26		76.26 ± 0.26		86.74 ± 0.26		88.71 ± 0.26		84.50 ± 0.26		89.25 ± 0.26
H (wt.%)		4.38 ± 0.41		8.94 ± 0.41		13.62 ± 0.41		14.35 ± 0.41		13.35 ± 0.41		14.46 ± 0.41
O (wt.%)		24.40 ± 0.94		13.28 ± 0.94		0.00 ± 0.94		0.00 ± 0.94		2.84 ± 0.94		0 ± 0.94
N (wt.%)		2.11 ± 0.05		1.06 ± 0.05		0.20 ± 0.05		0.11 ± 0.05		0.24 ± 0.05		0 ± 0.05
HHV (MJ/kg)		26.51 ± 0.26		35.96 ± 0.26	+(5)	46.34 ± 0.26	+(5)	48.75 ± 0.26	+(5)	45.20 ± 0.26	+(5)	49.02 ± 0.26
Biocrude elemental analysis and calorific value												
C (wt.%)		72.21 ± 0.95		62.20 ± 0.95		67.71 ± 0.95		66.44 ± 0.95		74.62 ± 0.95		69.76 ± 0.95
H (wt.%)		7.65 ± 0.16		9.05 ± 0.16		9.79 ± 0.16		9.08 ± 0.16		11.30 ± 0.16		9.33 ± 0.16
O (wt.%)		18.07 ± 1.20		29.44 ± 1.20		22.64 ± 1.20		24.24 ± 1.20		13.83 ± 1.20		20.06 ± 1.20
N (wt.%)		1.85 ± 0.28		0.54 ± 0.28		0.64 ± 0.28		0.88 ± 0.28		0.54 ± 0.28		1.01 ± 0.28
HHV (MJ/kg)	+(5)	32.58 ± 0.76	+(5)	27.98 ± 0.76		32.11 ± 0.76		30.86 ± 0.76	+(5)	37.75 ± 0.76	+(5)	33.18 ± 0.76
Biocrude chemical composition (Area %)												
Ketones		39.16 ± 1.18		27.38 ± 1.18		2.73 ± 1.18		8.66 ± 1.18		0.55 ± 1.18		5.38 ± 1.18
Phenols		50.79 ± 0.93		36.62 ± 0.93		4.46 ± 0.93		1.00 ± 0.93		5.38 ± 0.93		12.22 ± 0.93
Cyclic alkanes		0.00 ± 0.00		0.00 ± 0.00		3.17 ± 0.00		2.98 ± 0.00		5.31 ± 0.00		2.48 ± 0.00
Alkanes		0.45 ± 0.00		0.13 ± 0.00		8.57 ± 0.00		9.04 ± 0.00		20.84 ± 0.00		10.27 ± 0.00
Alkenes		1.37 ± 1.21		5.88 ± 1.21		4.68 ± 1.21		6.78 ± 1.21		1.89 ± 1.21		6.14 ± 1.21
Aromatic compounds		0.48 ± 0.74		12.59 ± 0.74		75.99 ± 0.74		68.59 ± 0.74		63.77 ± 0.74		58.57 ± 0.74
Carboxylic acids		0.00 ± 1.34		5.31 ± 1.34		0.30 ± 1.34		1.80 ± 1.34		0.73 ± 1.34		4.62 ± 1.34
Nitrogen compounds		10.76 ± 0.91		10.59 ± 0.91		0.19 ± 0.91		0.38 ± 0.91		0.00 ± 0.91		0.00 ± 0.91
FER (%)		79.87		71.48		98.76		97.48		96.90		83.40

Objectives: + and – account for maximising and minimising, respectively. Numbers in brackets are optimisation relative importances.

95% confidence for all the models, thus allowing their use for prediction purposes within the experimental interval of variation for the processing variables used in this work. Besides, the theoretical predictions obtained in Opt. 5 have been checked experimentally, and there are no significant differences between the experimental and predicted data with 95% confidence. Table S4 compares the experimental data and the predicted data for the 18 experiments conducted. For these data, the experimental values are not significantly different from those predicted by the models with 95% confidence. These data confirm the accurate predictivity of these models.

Opt.1 comprises the production of a biocrude with a high HHV. Opt.2 is also directed towards an energy-dense biocrude and maximises the amount of disposable face masks in the feedstock. Opt. 3 and Opt. 4 include the production of an energy-dense solid biofuel (maximising the yield and HHV of the hydrochar) without any feedstock restriction and minimising the proportion of disposable face masks in the feedstock, respectively. Opt. 5 comprises the simultaneous production of energy-dense liquid (biocrude) and solid (hydrochar) biofuels, maximising the yields and HHV of these products, with Opt.6 including the same restrictions and minimising the amount of disposable face masks. For these optima, a relative importance (from least important 1, to most important, 5) has been given to each constraint to develop processing conditions that adequately satisfy all criteria.

Regarding liquid biofuels, Opt.1 shows that the highest production (26% yield) of an energy-dense biocrude (32 MJ/kg) occurs by processing almond hulls in deionised water for 115 min. Opt.2 reveals that the feedstock could comprise up to 20% of face masks without substantially modifying the quantity (22% yield) and quality (28 MJ/kg) of the biocrude produced. For this, the process must be conducted with 5 wt% seawater (equivalent to a reaction medium salinity of 2235 ppm) for 95 min. In both scenarios, theoretical feedstock energy recoveries higher than 70% are achieved. For solid biofuels, Opt.3 shows that an energetic-like (46 MJ/kg) hydrochar can be produced in high yield (83%) with a mixture comprising 8:92 (wt.%) almond hulls/disposable face masks in a reaction medium including 84:16 (wt.%) seawater/deionised water (equivalent to reaction medium salinity of 37471 ppm) for 180 min. In parallel, Opt. 4 reveals that up to 27 wt% almond hulls can be co-processed with face masks without substantially decreasing the quantity (65% yield) and fuel quality (49 MJ/kg) of the hydrochar produced, using a water mixture comprising 95:5 (wt.%) seawater/deionised water (equivalent to reaction medium salinity of 42378 ppm) for 180 min. These conditions allow for theoretical feedstock energy recovery higher than 97% in these two latter cases. Concerning liquid and solid biofuels production, energy-dense biocrude (12% yield, HHV = 38 MJ/kg) and hydrochar (86% yield, HHV = 45 MJ/kg) can be produced concurrently from disposable face masks conducting the process with seawater (salinity of 44608 ppm) for 180 min, with a feedstock energy recovery close to 97%. This biofuels production can be maintained, including up to 22 wt% almond hulls in the feedstock (Opt. 6). When this mixture is treated with seawater for 147 min, 13% is converted to biocrude (33 MJ/kg) and 67% to hydrochar (49 MJ/kg), leading to a theoretical feedstock energy recovery of 83%.

3.7. Limitations and recommendations for future work

The promising results of this research might lay the first stone in future renewable and sustainable energy production via biomass-plastic co-valorisation. This allows a more efficient conversion of biomass into drop-in biofuels while reducing pollution challenges due to using waste plastic materials as co-feeding materials. Besides, the total and/or partial substitution of freshwater with seawater improves the sustainability of hydrothermal processes as this valorisation route could be unsustainable in some regions with a freshwater shortage. Additionally, it could encourage the energy industry's progressive transition towards a greener and more sustainable energy market, allowing an efficient and concurrent 'decarbonisation and deplastification' of the planet. This thinking might also contribute to developing future holistic biorefineries based on new and exciting synergetic interactions between materials rather than a simple concatenation of operating units specifically designed for one kind of feedstock. Due to the presence of plastic waste in various ecosystems, this idea can be regarded as a novel strategy to combat earth and sea pollution simultaneously, thus being a step forward towards the energy of the future while facing the pollution challenges of the present. This work has used almond hulls and disposable face masks as representatives of lignocellulosic biomass and plastic materials as a proof of concept. In this sense, it must be borne in mind that different synergies could arise between the processing materials depending on the feedstock and reaction medium. Although these might be checked experimentally, our procedure and strategy will continue to be valid and could help researchers address different co-valorisation challenges between different biomasses and plastic materials. It is also important to note that the optimised processing conditions of this work provide a good approximation of optimum values for these feedstocks under the reaction conditions tested and the type of reactor used. Consequently, for possible future implementation and commercialisation, these conditions must be experimentally corroborated as slight differences may arise due to differences in the feedstock composition (disposable face masks and almond hulls) and/or the type/dimensions of the reactor used. Additionally, the chemical composition of seawater varies from sea to sea. This can also influence this process and is worth investigating. For example, different types of seawater with varying chemical compositions could be used to determine the species responsible for the promoting effects occurring during the HTT of biomass and plastics.

4. Conclusions

This work has explored the hydrothermal co-valorisation of almond hulls and disposable face masks using different water (deionised and seawater) mixtures and processing times (20–180 min). Synergistic and antagonistic interactions between these feedstocks combined with several promoting and inhibiting effects displayed by seawater influenced the overall distribution of reaction products and their physicochemical and fuel properties. In particular, bilateral synergies between almond hulls and face masks promoted the formation of biocrude and aqueous products at the expense of the production of gas and hydrochar. Notably, the decomposition of almond hulls released active fragments, which behaved as active donors aiding face masks decomposition via chain scission. This boosted the production of reactive H fragments from face masks, which stabilised the free radicals produced from almond hulls. In parallel, seawater also promoted biocrude formation favouring the scission of O–H bonds in almond hulls, although it did not show any catalytic capability for the C–C scissions needed for face masks depolymerisation. This reaction medium could also counter some biomass-plastic negative influences, as it promoted different chemical transformations that helped palliate these negative influences. Process optimisation revealed that the relationship between almond hulls and disposable face masks and the deionised water/seawater ratio (water salinity) can be effectively controlled to produce energy-dense liquid and solid biofuels, individually and/or concurrently to suit different market needs, ensuring a sustainable and efficient co-valorisation of food waste and plastic residues.

Declaration of Competing Interest

The authors declare that they have no known competing financial interests or personal relationships that could have appeared to influence the work reported in this paper.

Data availability

Data will be made available on request.

Acknowledgements

This work was funded by FEDER and the Spanish Ministry of Science, Innovation and Universities (ENE 2017-83854-R) and MCIN/AEI/10.13039/501100011033 (I+D+i project PID2020-115053RB-I00). Javier Remón is grateful to the Spanish Ministry of Science, Innovation and Universities for the Juan de la Cierva (JdC) fellowship (IJC2018-037110-I) awarded.

Appendix A. Supplementary data

Supplementary data to this article can be found online at https://doi.org/10.1016/j.cej.2022.137810.

References

[1] T.M. Attard, J.H. Clark, C.R. McElroy, Recent developments in key biorefinery areas, Curr. Opin. Green Sustain. Chem. 21 (2020) 64–74, https://doi.org/10.1016/j.cogsc.2019.12.002.
[2] J.H. Clark, Green biorefinery technologies based on waste biomass, Green Chem. 21 (6) (2019) 1168–1170, https://doi.org/10.1039/C9GC90021G.
[3] A.J. Esfahlan, R. Jamei, R.J. Esfahlan, The importance of almond (Prunus amygdalus L.) and its by-products, Food Chem. 120 (2) (2010) 349–360.
[4] J. Remón, R. Sevilla-Gasca, E. Frecha, J.L. Pinilla, I. Suelves, Direct conversion of almond waste into value-added liquids using carbon-neutral catalysts: hydrothermal hydrogenation of almond hulls over a Ru/CNF catalyst, Sci. Total Environ. 825 (2022), 154044, https://doi.org/10.1016/j.scitotenv.2022.154044.
[5] M.S. Seshasayee, P.E. Savage, Synergistic interactions during hydrothermal liquefaction of plastics and biomolecules, Chem. Eng. J. 417 (2021) 129268.
[6] S. Hongthong, S. Raikova, H.S. Leese, C.J. Chuck, Co-processing of common plastics with pistachio hulls via hydrothermal liquefaction, Waste Manag. 102 (2020) 351–361, https://doi.org/10.1016/j.wasman.2019.11.003.
[7] S. Jung, S. Lee, X. Dou, E.E. Kwon, Valorization of disposable COVID-19 mask through the thermo-chemical process, Chem. Eng. J. 405 (2021), 126658, https://doi.org/10.1016/j.cej.2020.126658.
[8] J. Yang, Q. He, L. Yang, A review on hydrothermal co-liquefaction of biomass, Appl. Energy 250 (2019) 926–945, https://doi.org/10.1016/j.apenergy.2019.05.033.
[9] M. Kumar, A. Olajire Oyedun, A. Kumar, A review on the current status of various hydrothermal technologies on biomass feedstock, Renew. Sust. Energ. Rev. 81 (2018) 1742–1770, https://doi.org/10.1016/j.rser.2017.05.270.
[10] J. Remón, J. Randall, V.L. Budarin, J.H. Clark, Production of bio-fuels and chemicals by microwave-assisted, catalytic, hydrothermal liquefaction (MAC-HTL) of a mixture of pine and spruce biomass, Green Chem. 21 (2) (2019) 284–299, https://doi.org/10.1039/c8gc03244k.
[11] A. Dimitriadis, S. Bezergianni, Hydrothermal liquefaction of various biomass and waste feedstocks for biocrude production: a state of the art review, Renew Sust Energ Rev 68 (2017) 113–125, https://doi.org/10.1016/j.rser.2016.09.120.
[12] J.A. Okolie, E.I. Epelle, S. Nanda, D. Castello, A.K. Dalai, J.A. Kozinski, Modeling and process optimization of hydrothermal gasification for hydrogen production: a comprehensive review, J. Supercritical Fluids 173 (2021) 105199.
[13] K. Sharma, D. Castello, M.S. Haider, T.H. Pedersen, L.A. Rosendahl, Continuous co-processing of HTL bio-oil with renewable feed for drop-in biofuels production for sustainable refinery processes, Fuel 306 (2021) 121579.
[14] D.C. Elliott, P. Biller, A.B. Ross, A.J. Schmidt, S.B. Jones, Hydrothermal liquefaction of biomass: developments from batch to continuous process, Bioresour. Technol. 178 (2015) 147–156, https://doi.org/10.1016/j.biortech.2014.09.132.
[15] S.S. Toor, L. Rosendahl, A. Rudolf, Hydrothermal liquefaction of biomass: A review of subcritical water technologies, Energy 36 (5) (2011) 2328–2342, https://doi.org/10.1016/j.energy.2011.03.013.
[16] A.R.K. Gollakota, N. Kishore, S. Gu, A review on hydrothermal liquefaction of biomass, Renew. Sustain. Energ. Rev. 81 (2018) 1378–1392, https://doi.org/10.1016/j.rser.2017.05.178.
[17] J. Remón, A.S. Matharu, J.H. Clark, Simultaneous production of lignin and polysaccharide rich aqueous solutions by microwave-assisted hydrothermal treatment of rapeseed meal, Energy Convers. Manage. 165 (2018) 634–648, https://doi.org/10.1016/j.enconman.2018.03.091.
[18] B.J. He, Y. Zhang, T.L. Funk, G.L. Riskowski, Y. Yin, Thermochemical conversion of swine mamure: an alternative process for waste treatment and renewable energy production, Trans. Am. Soc. Agric. Eng. 43 (6) (2000) 1827–1833, https://doi.org/10.13031/2013.3087.
[19] T. Minowa, M. Murakami, Y. Dote, T. Ogi, S.Y. Yokoyama, Oil production from garbage by thermochemical liquefaction, Biomass Bioenerg 8 (2) (1995) 117–120, https://doi.org/10.1016/0961-9534(95)00017-2.
[20] S. Karagöz, T. Bhaskar, A. Muto, Y. Sakata, Comparative studies of oil compositions produced from sawdust, rice husk, lignin and cellulose by hydrothermal treatment, Fuel 84 (7–8) (2005) 875–884, https://doi.org/10.1016/j.fuel.2005.01.004.
[21] A. Demirbaş, Thermochemical conversion of biomass to liquid products in the aqueous medium, Energy Sources 27 (13) (2005) 1235–1243, https://doi.org/10.1080/009083190519357.
[22] J. Remón, J. Latorre-Viu, A.S. Matharu, J.L. Pinilla, I. Suelves, Analysis and optimisation of a novel 'almond-refinery' concept: simultaneous production of biofuels and value-added chemicals by hydrothermal treatment of almond hulls, Sci. Total Environ. 765 (2021), 142671, https://doi.org/10.1016/j.scitotenv.2020.142671.
[23] B. Bai, H. Jin, C. Fan, C. Cao, W. Wei, W. Cao, Experimental investigation on liquefaction of plastic waste to oil in supercritical water, Waste Manag. 89 (2019) 247–253, https://doi.org/10.1016/j.wasman.2019.04.017.
[24] X. Zhao, Y. Xia, L. Zhan, B. Xie, B. Gao, J. Wang, Hydrothermal treatment of E-Waste plastics for tertiary recycling: product slate and decomposition mechanisms, ACS Sustain. Chem. Eng. 7 (1) (2018) 1464–1473, https://doi.org/10.1021/acssuschemeng.8b05147.
[25] T. Helmer Pedersen, F. Conti, Improving the circular economy via hydrothermal processing of high-density waste plastics, Waste Manag. 68 (2017) 24–31, https://doi.org/10.1016/j.wasman.2017.06.002.
[26] M.S. Seshasayee, P.E. Savage, Oil from plastic via hydrothermal liquefaction: production and characterization, Appl. Energy 278 (2020) 115673.
[27] S. Hongthong, H.S. Leese, C.J. Chuck, Valorizing plastic-contaminated waste streams through the catalytic hydrothermal processing of polypropylene with lignocellulose, ACS Omega 5 (32) (2020) 20586–20598, https://doi.org/10.1021/acsomega.0c02854.
[28] S. Raikova, T.D.J. Knowles, M.J. Allen, C.J. Chuck, Co-liquefaction of macroalgae with common marine plastic pollutants, ACS Sustain. Chem. Eng. 7 (7) (2019) 6769–6781, https://doi.org/10.1021/acssuschemeng.8b06031.
[29] B. Wang, Y. Huang, J. Zhang, Hydrothermal liquefaction of lignite, wheat straw and plastic waste in sub-critical water for oil: product distribution, J. Anal. Appl. Pyrolysis 110 (2014) 382–389, https://doi.org/10.1016/j.jaap.2014.10.004.
[30] X. Yuan, H. Cao, H. Li, G. Zeng, J. Tong, L. Wang, Quantitative and qualitative analysis of products formed during co-liquefaction of biomass and synthetic polymer mixtures in sub- and supercritical water, Fuel Process. Technol. 90 (3) (2009) 428–434, https://doi.org/10.1016/j.fuproc.2008.11.005.
[31] P. Bhattacharya, P.H. Steele, E.B.M. Hassan, B. Mitchell, L. Ingram, C. U. Pittman Jr, Wood/plastic copyrolysis in an auger reactor: chemical and physical analysis of the products, Fuel 88 (7) (2009) 1251–1260, https://doi.org/10.1016/j.fuel.2009.01.009.
[32] B. Cao, Y. Sun, J. Guo, S. Wang, J. Yuan, S. Esakkimuthu, B. Bernard Uzoejinwa, C. Yuan, A.-E.-F. Abomohra, L. Qian, L. Liu, B. Li, Z. He, Q. Wang, Synergistic effects of co-pyrolysis of macroalgae and polyvinyl chloride on bio-oil/bio-char properties and transferring regularity of chlorine, Fuel 246 (2019) 319–329, https://doi.org/10.1016/j.fuel.2019.02.037.
[33] J. Remón, S.H. Danby, J.H. Clark, A.S. Matharu, A new step forward nonseasonal 5G biorefineries: microwave-assisted, synergistic, Co-depolymerization of wheat straw (2G Biomass) and Laminaria saccharina (3G Biomass), ACS Sustain. Chem. Eng. 8 (33) (2020) 12493–12510, https://doi.org/10.1021/acssuschemeng.0c03390.
[34] J. Remón, P. Arcelus-Arrillaga, L. García, J. Arauzo, Simultaneous production of gaseous and liquid biofuels from the synergetic co-valorisation of bio-oil and crude glycerol in supercritical water, Appl. Energy 228 (2018) 2275–2287, https://doi.org/10.1016/j.apenergy.2018.07.093.
[35] A.A. Shah, K. Sharma, M.S. Haider, S.S. Toor, L.A. Rosendahl, T.H. Pedersen, D. Castello, The role of catalysts in biomass hydrothermal liquefaction and biocrude upgrading, Processes 10 (2) (2022), https://doi.org/10.3390/pr10020207.
[36] Z. Jiang, V.L. Budarin, J. Fan, J. Remón, T. Li, C. Hu, J.H. Clark, Sodium chloride-assisted depolymerization of Xylo-oligomers to Xylose, ACS Sustain. Chem. Eng. 6 (3) (2018) 4098–4104, https://doi.org/10.1021/acssuschemeng.7b04463.
[37] J. Yang, N. Nasirian, H. Chen, H. Niu, Q. He, Hydrothermal liquefaction of sawdust in seawater and comparison between sodium chloride and sodium carbonate, Fuel 308 (2022) 122059.
[38] J. Yang, H. Chen, Q. Liu, N. Zhou, Y. Wu, Q. He, Is it feasible to replace freshwater by seawater in hydrothermal liquefaction of biomass for biocrude production? Fuel 282 (2020) 118870.
[39] L. Hu, Y. Luo, B. Cai, J. Li, D. Tong, C. Hu, The degradation of the lignin in Phyllostachys heterocycla cv. pubescens in an ethanol solvothermal system, Green Chem. 16 (6) (2014) 3107–3116.
[40] N.G.T. Meneses, S. Martins, J.A. Teixeira, S.I. Mussatto, Influence of extraction solvents on the recovery of antioxidant phenolic compounds from brewer's spent grains, Sep. Purif. Technol. 108 (2013) 152–158, https://doi.org/10.1016/j.seppur.2013.02.015.
[41] T. Aktas, P. Thy, R.B. Williams, Z. McCaffrey, R. Khatami, B.M. Jenkins, Characterization of almond processing residues from the Central Valley of California for thermal conversion, Fuel Process. Technol. 140 (2015) 132–147, https://doi.org/10.1016/j.fuproc.2015.08.030.
[42] J.F. González, C.M. González-García, A. Ramiro, J. Gañán, J. González, E. Sabio, S. Román, J. Turegano, Use of almond residues for domestic heating. Study of the combustion parameters in a mural boiler, Fuel Process. Technol. 86 (12-13) (2005) 1351–1368.
[43] J. Remón, M. Casales, J. Gracia, M.S. Callén, J.L. Pinilla, I. Suelves, Sustainable production of liquid biofuels and value-added platform chemicals by hydrodeoxygenation of lignocellulosic bio-oil over a carbon–neutral Mo2C/CNF catalyst, Chem. Eng. J. 405 (2021) 126705, https://doi.org/10.1016/j.cej.2020.126705.
[44] S. Ren, X.P. Ye, A.P. Borole, Separation of chemical groups from bio-oil water-extract via sequential organic solvent extraction, J. Anal. Appl. Pyrolysis 123 (2017) 30–39, https://doi.org/10.1016/j.jaap.2017.01.004.

[45] S.A. Channiwala, P.P. Parikh, A unified correlation for estimating HHV of solid, liquid and gaseous fuels, Fuel 81 (8) (2002) 1051–1063, https://doi.org/10.1016/s0016-2361(01)00131-4.
[46] X. Ding, S. Mahadevan Subramanya, T. Fang, Y. Guo, P.E. Savage, Effects of potassium phosphates on hydrothermal liquefaction of triglyceride, protein, and polysaccharide, Energy Fuels 34 (12) (2020) 15313–15321.
[47] U. Jena, K.C. Das, J.R. Kastner, Comparison of the effects of Na_2CO_3, $Ca_3(PO_4)_2$, and NiO catalysts on the thermochemical liquefaction of microalga Spirulina platensis, Appl. Energy 98 (2012) 368–375, https://doi.org/10.1016/j.apenergy.2012.03.056.
[48] C. Xu, J. Lancaster, Conversion of secondary pulp/paper sludge powder to liquid oil products for energy recovery by direct liquefaction in hot-compressed water, Water Res. 42 (6–7) (2008) 1571–1582, https://doi.org/10.1016/j.watres.2007.11.007.
[49] D. Castello, L. Fiori, Supercritical water gasification of biomass: a stoichiometric thermodynamic model, Int. J. Hydrogen Energy 40 (21) (2015) 6771–6781, https://doi.org/10.1016/j.ijhydene.2015.03.120.
[50] J. Remón, F. Ravaglio-Pasquini, L. Pedraza-Segura, P. Arcelus-Arrillaga, I. Suelves, J.L. Pinilla, Caffeinating the biofuels market: effect of the processing conditions during the production of biofuels and high-value chemicals by hydrothermal treatment of residual coffee pulp, J. Clean. Prod. 302 (2021) 127008, https://doi.org/10.1016/j.jclepro.2021.127008.
[51] A. Demirbaş, Mechanisms of liquefaction and pyrolysis reactions of biomass, Energy Convers. Manage. 41 (6) (2000) 633–646, https://doi.org/10.1016/S0196-8904(99)00130-2.
[52] D. Castello, A. Kruse, L. Fiori, Biomass gasification in supercritical and subcritical water: the effect of the reactor material, Chem. Eng. J. 228 (2013) 535–544, https://doi.org/10.1016/j.cej.2013.04.119.
[53] S. Thiruvenkadam, S. Izhar, H. Yoshida, M.K. Danquah, R. Harun, Process application of Subcritical Water Extraction (SWE) for algal bio-products and biofuels production, Appl. Energy 154 (2015) 815–828, https://doi.org/10.1016/j.apenergy.2015.05.076.
[54] P. Duan, X. Bai, Y. Xu, A. Zhang, F. Wang, L. Zhang, J. Miao, Catalytic upgrading of crude algal oil using platinum/gamma alumina in supercritical water, Fuel 109 (2013) 225–233, https://doi.org/10.1016/j.fuel.2012.12.074.
[55] P. Duan, P.E. Savage, Catalytic hydrotreatment of crude algal bio-oil in supercritical water, Appl. Catal. B: Environ. 104 (1-2) (2011) 136–143.
[56] P. Duan, P.E. Savage, Catalytic treatment of crude algal bio-oil in supercritical water: optimization studies, Energy Environ. Sci. 4 (4) (2011) 1447, https://doi.org/10.1039/c0ee00343c.
[57] C.A. Fisk, T. Morgan, Y. Ji, M. Crocker, C. Crofcheck, S.A. Lewis, Bio-oil upgrading over platinum catalysts using in situ generated hydrogen, Appl. Catal. A: General 358 (2) (2009) 150–156.
[58] R.B. Madsen, R.Z.K. Bernberg, P. Biller, J. Becker, B.B. Iversen, M. Glasius, Hydrothermal co-liquefaction of biomasses – quantitative analysis of bio-crude and aqueous phase composition, Sustain. Energy Fuels 1 (4) (2017) 789–805, https://doi.org/10.1039/c7se00104e.
[59] J. Shabaker, Aqueous-phase reforming of methanol and ethylene glycol over alumina-supported platinum catalysts, J. Catal. 215 (2) (2003) 344–352, https://doi.org/10.1016/s0021-9517(03)00032-0.